18 Micromeritics

Chapter Objectives

At the conclusion of this chapter the student should be able to:

1. Understand the concept of particle size as it applies to the pharmaceutical sciences.
2. Discuss the common particle sizes of pharmaceutical preparations and their impact on pharmaceutical processing/preparation.
3. Be familiar with the units for particle size, area, and volume and typical calculations.
4. Describe how particles can be characterized and why these methods are important.
5. Discuss the methods for determining particle size.
6. Discuss the role and importance of particle shape and surface area.
7. Understand the methods for determining particle surface area.
8. State the two fundamental properties for any collection of particles.
9. Describe what a derived property of a powder is and identify the important derived properties.

Knowledge and control of the size and the size range of particles are of profound importance in pharmacy. Thus, size, and hence surface area, of a particle can be related in a significant way to the physical, chemical, and pharmacologic properties of a drug. Clinically, the particle size of a drug can affect its release from dosage forms that are administered orally, parenterally, rectally, and topically. The successful formulation of suspensions, emulsions, and tablets, from the viewpoints of both physical stability and pharmacologic response, also depends on the particle size achieved in the product. In the area of tablet and capsule manufacture, control of the particle size is essential in achieving the necessary flow properties and proper mixing of granules and powders. These and other factors reviewed by Lees1 make it apparent that a pharmacist today must possess a sound knowledge of micromeritics.

Particle Size and Size Distribution

In a collection of particles of more than one size (in other words, in a polydisperse sample), two properties are important, namely, (*a*) the shape and surface area of the individual particles and (*b*) the size range and number or weight of particles present and, hence, the total surface area. Particle size and size distributions will be considered in this section; shape and surface area will be discussed subsequently.

Key Concept

Micromeritics

The science and technology of small particles was given the name *micromeritics* by Dalla Valle.2 Colloidal dispersions are characterized by particles that are too small to be seen in the ordinary microscope, whereas the particles of pharmaceutical emulsions and suspensions and the “fines” of powders fall in the range of the optical microscope. Particles having the size of coarser powders, tablet granulations, and granular salts fall within the sieve range. The approximate size ranges of particles in pharmaceutical dispersions are listed in Table 18-1. The sizes of other materials, including microorganisms, are given in Tables 18-2 and 18-3. The unit of particle size used most frequently in micromeritics is the micrometer, μm, also called the micron, μ, and equal to 10^{-6} m, 10^{-4} cm, and 10^{-3} mm. One must not confuse μm with mμ, the latter being the symbol for a millimicron or 10^{-9} m. The millimicron now is most commonly referred to as the nanometer (nm).

The size of a sphere is readily expressed in terms of its diameter. As the degree of asymmetry of particles increases, however, so does the difficulty of expressing size in terms of a meaningful diameter. Under these conditions, there is no one unique diameter for a particle. Recourse must be made to the use of an *equivalent spherical diameter*, which relates the size of the particle to the diameter of a sphere having the same surface area, volume, or diameter. Thus, the surface diameter, d_s, is the diameter of a

sphere having the same surface area as the particle in question. The diameter of a sphere having the same volume as the particle is the volume diameter, d_v, whereas the projected diameter, d_p, is the diameter of a sphere having the same observed area as the particle when viewed normal to its most stable plane. The size can also be expressed as the Stokes diameter, d_{st}, which describes an equivalent sphere undergoing sedimentation at the same rate as the asymmetric particle. Invariably, the type of diameter used reflects the method employed to obtain the diameter. As will be seen later, the projected diameter is obtained by microscopic techniques, whereas the Stokes diameter is determined from sedimentation studies on the suspended particles.

P.443

Table 18-1 Particle Dimensions in Pharmaceutical Disperse Systems

Particle Size, Diameter			
Micrometers (μm)	**Millimeters**	**Approximate Sieve Size**	**Examples**
0.5–10	0.0005–0.010	–	Suspensions, fine emulsions
10–50	0.010–0.050	–	Upper limit of subsieve range, coarse emulsion particles; flocculated suspension particles
50–100	0.050–0.100	325–140	Lower limit of sieve range, fine powder range
150–1000	0.150–1.000	100–18	Coarse powder range
1000–3360	1.000–3.360	18–6	Average granule size

Any collection of particles is usually polydisperse. It is therefore necessary to know not only the size of a certain particle but also how many particles of the same size exist in the sample. Thus, we need an estimate of the size range present and the number or weight fraction of each particle size. This is the particle-size distribution, and from it we can calculate an average particle size for the sample.

If a drug product formulator desires to work with particles of approximately uniform size (i.e., *monodisperse* rather than*polydisperse*), he or she may obtain batches of latex particles as small as 0.060 μm (60 nm) in diameter with a standard deviation, σ, of ±0.012 μm and particles as large as 920 μm (0.920 nm) with σ = ±32.50. Such particles of uniform size3 are used in science, medicine, and technology for various diagnostic tests; as particle-size standards for particle analyzers; for the accurate determination of pore sizes in filters; and as uniformly sized surfaces upon which antigens can be coated for effective immunization. Nanosphere Size Standards4 are available in 22 sizes, from 21 nm (0.021 μm) to 900 nm (0.9 μm or 0.0009 mm) in diameter for instrument calibration and quality control in the manufacture of submicron-sized products such as liposomes, nanoparticles, and microemulsions.

Average Particle Size

Suppose we have conducted a microscopic examination of a sample of a powder and recorded the number of particles lying within various size ranges. Data from such a determination are shown in Table 18-4. To compare these values with those from, say, a second batch of the same material, we

P.444

P.445

usually compute an average or mean diameter as our basis for comparison.

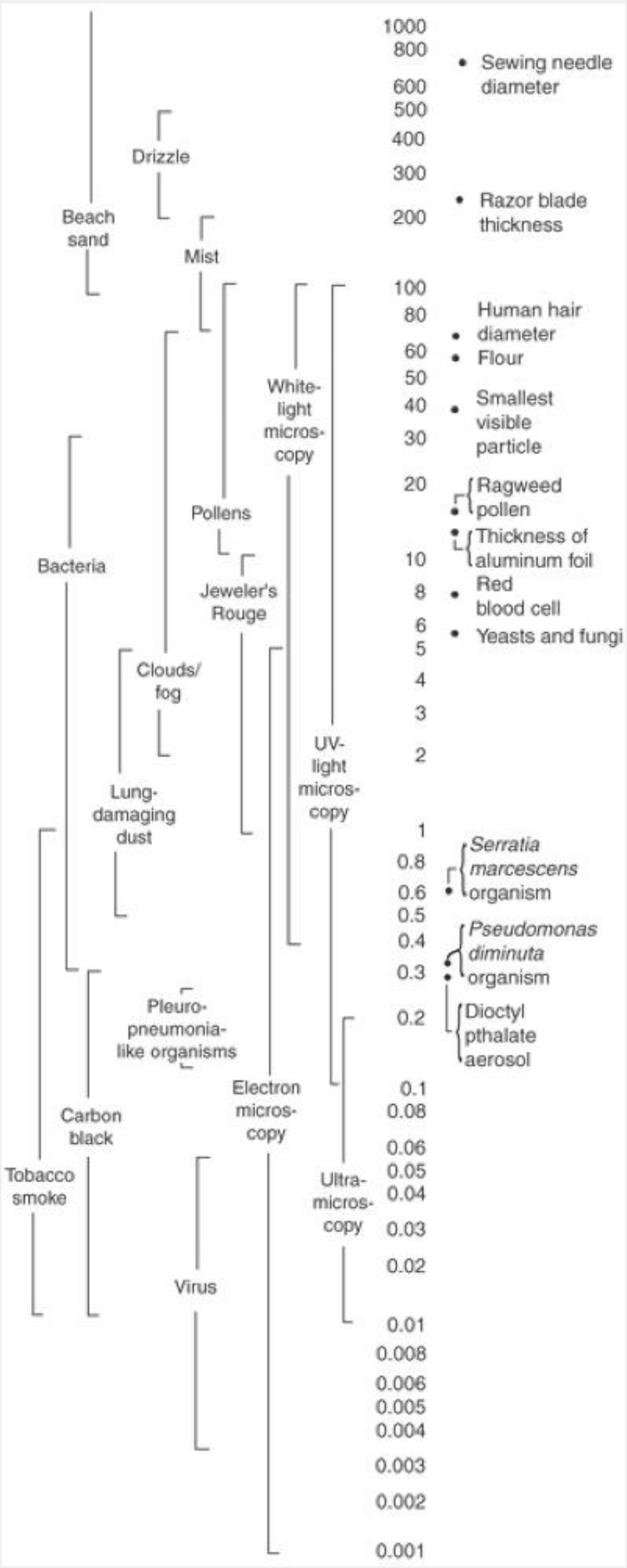
1000
800
600
500
400
300
200
100
80
60
50
40
30
20
10
8
6
5
4
3
2
1
0.8
0.6
0.5
0.4
0.3
0.2
0.1
0.08
0.06
0.05
0.04
0.03
0.02
0.01
0.008
0.006
0.005
0.004
0.003
0.002
0.001
Sewing needle diameter
Razor blade thickness
Human hair diameter
Flour
Smallest visible particle
Ragweed pollen
Thickness of aluminum foil
Red blood cell
Yeasts and fungi
Serratia marcescens organism
Pseudomonas diminuta organism
Dioctyl pthalate aerosol
Beach sand
Drizzle
Mist
Pollens
Bacteria
Clouds/ fog
Lung-damaging dust
Jeweler's Rouge
White-light micros-copy
UV-light micros-copy
Pleuro-pneumonia-like organisms
Carbon black
Tobacco smoke
Virus
Electron micros-copy
Ultra-micros-copy

Table 18-2 A Scale of the Ranges of Various Small Particles, Together with the Wavelength of Light and Other Electromagnetic Waves That Illuminate Materials Found in These Size Ranges

Table 18-3 ROD Length and Diameter of Various Microorganisms

Organism	Rod Length (µm)	Rod or Coccus Diameter (µm)	Significance
Acetobacter melanogenus	1.0–2.0	0.4–0.8	Strong beer/vinegar bacterium
Alcaligenes viscolactis	0.8–2.6	0.6–1.0	Causes ropiness in milk
Bacillus anthracis	3.0–10.0	1.0–1.3	Causes anthrax in mammals
B. stearothermophilus	2.0–5.0	0.6–1.0	Biologic indicator for steam sterilization
B. subtilis	2.0–3.0	0.7–0.8	Biologic indicator for ethylene oxide sterilization
Clostridium botulinum (B)	3.0–8.0	0.5–0.8	Produces exotoxin causing botulism
C. perfringens	4.0–8.0	1.0–1.5	Produces toxin causing food poisoning
C. tetani	4.0–8.0	0.4–0.6	Produces exotoxin causing tetanus
Diplococcus pneumoniae		0.5–1.25	Causes lobar pneumonia
Erwinia aroideae	2.0–3.0	0.5	Causes soft rot in vegetables

Escherichia coli	1.0–3.0	0.5	Indicator of fecal contamination in water
Haemophilus influenzae	0.5–2.0	0.2–0.3	Causes influenza and acute respiratory infections
Klebsiella pneumoniae	5.0	0.3–0.5	Causes pneumonia and other respiratory inflammations
Lactobacillus delbrueckii	2.0–9.0	0.5–0.8	Causes souring of grain mashes
Leuconostoc mesenteroides		0.9–1.2	Causes slime in sugar solutions
Mycoplasma pneumoniae(PPLO)		0.3–0.5	Smallest known free-living organism
Pediococcus acidilactici		0.6–1.0	Causes mash spoilage in brewing
P. cerevisiae		1.0–1.3	Causes deterioration in beer
Pseudomonas diminuta	1.0	0.3	Test organism for retention of 0.2-µm membranes
Salmonella enteritidis	2.0–3.0	0.6–0.7	Causes food poisoning
S. hirschfeldii	1.0–2.5	0.3–0.5	Causes enteric fever
S. typhimurium	1.0–1.5	0.5	Causes food poisoning in humans

S. typhosa	2.0–3.0	0.6–0.7	Causes typhoid fever
Sarcina maxima		4.0–4.5	Isolated from fermenting malt mash
Serratia marcescens	0.5–1.0	0.5	Test organism for retention of 0.45-µm membranes
Shigella dysenteriae	1.0–3.0	0.4–0.6	Causes dysentery in humans
Staphylococcus aureus		0.8–1.0	Causes pus-forming infections
Streptococcus lactis		0.5–1.0	Contaminant in milk
S. pyogenes		0.6–1.0	Causes pus-forming infections
Vibrio percolans	1.5–1.8	0.3–0.4	Test organism for retention of 0.2-µm membranes

Table 18-4 Calculation of Statistical Diameters from Data Obtained by Use of the Microscopic Method (Normal Distribution)

Size Range (µm)	Mean of Size Range (µm)	Number of Particles in Each Size Range, n	nd	nd^2	nd^3	nd^4
0.50–1.00	0.75	2	1.50	1.13	0.85	0.64
1.00–1.50	1.25	10	12.50	15.63	19.54	24.43
1.50–2.00	1.75	22	38.50	67.38	117.92	206.36
2.00–2.50	2.25	54	121.50	273.38	615.11	1384.00
2.50–3.00	2.75	17	46.75	128.56	353.54	972.24
3.00–3.50	3.25	8	26.00	84.50	274.63	892.55
3.50–4.00	3.75	5	18.75	70.31	263.66	988.73
		$\sum n$= 118	$\sum nd$ = 265.50	$\sum nd^2$= 640.89	$\sum nd^3$ = 1645.25	$\sum nd^4$ = 4468.95

TABLE 18–5
STATISTICAL DIAMETERS*

$\left(\frac{\sum nd^{p+f}}{\sum nd^{f}}\right)^{1/p}$	p	f	Type of Mean	Size Parameter	Frequency	Mean Diameter	Value for Data in Table 18–4 (μm)	Comments
$\frac{\sum nd}{\sum n}$	1	0	Arithmetic	Length	Number	Length-number mean, d_{ln}	2.25	Satisfactory if size narrow and distri normal; these co are rarely found pharmaceutical p
$\sqrt{\frac{\sum nd^2}{\sum n}}$	2	0	Arithmetic	Surface	Number	Surface-number mean, d_{sn}	2.33	Refers to particle h average surface a
$\sqrt{\frac{\sum nd^3}{\sum n}}$	3	0	Arithmetic	Volume	Number	Volume-number mean, d_{vn}	2.41	Refers to particle h average weight a related inversely number of partic gram of material
$\frac{\sum nd^2}{\sum nd}$	1	1	Arithmetic	Length	Length	Surface-length or length-weighted mean, d_{sl}	2.41	No practical signifi
$\frac{\sum nd^3}{\sum nd^2}$	1	2	Arithmetic	Length	Surface	Volume-surface or surface-weighted mean, d_{vs}	2.57	Important pharmac because inversely to S_w, the specifi
$\frac{\sum nd^4}{\sum nd^3}$	1	3	Arithmetic	Length	Weight	Weight-moment or volume-weighted mean, d_{wm}	2.72	Limited pharmaceu significance

*Modified from I. C. Edmundson, in H. S. Bean, J. E. Carless, and A. H. Beckett (Eds.), *Advances in Pharmaceutical Sciences*, Vol. 2, Academic Press, Lon p. 950. With permission.

Table 18-5 Statistical Diameters*

Edmundson5 derived a general equation for the average particle size, whether it be an arithmetic, a geometric, or a harmonic mean diameter:

$$d_{\text{mean}} = \left(\frac{\sum nd^{p+f}}{\sum nd^{f}}\right)^{1/p} \qquad \textbf{(18–1)}$$

In equation **(**18-1**)**, n is the number of particles in a size range whose midpoint, d, is one of the equivalent diameters mentioned previously. The term p is an index related to the size of an individual particle, because d raised to the power $p = 1$, $p = 2$, or $p = 3$ is an expression of the particle length, surface, or volume, respectively. The value of the index p also decides whether the mean is arithmetic (p is positive), geometric (p is zero), or harmonic (p is negative). For a collection of particles, the frequency with which a particle in a certain size range occurs is expressed by nd^f. When the frequency index, f, has values of 0, 1, 2, or 3, then the size frequency distribution is expressed in terms of the total number, length, surface, or volume of the particles, respectively.

Some of the more significant arithmetic (p is positive) mean diameters are shown in Table 18-5. These are based on the values of p and f used in equation **(**18-1**)**. The diameters calculated from the data in Table 18-4 are also included. For a more complete description of these diameters, refer to the work of Edmundson.5

Particle-Size Distribution

When the number, or weight, of particles lying within a certain size range is plotted against the size range or mean particle size, a so-called *frequency distribution curve* is obtained. Typical examples are shown in Figures 18-1 (based on Table 18-4) and 18-2 (based onTable 18-6). Such plots give a visual representation of the distribution that an average diameter cannot achieve. This is important because it

is possible to have two samples with the same average diameter but different distributions. Moreover, it is immediately apparent from a frequency distribution curve what particle size occurs most frequently within the sample. This is termed the *mode*.
An alternative method of representing the data is to plot the cumulative percentage over or under a particular size versus
P.446

P.447

particle size. This is done in Figure 18-3, using the cumulative percent undersize (column 5, Table 18-6). A sigmoidal curve results, with the mode being that particle size at the greatest slope.

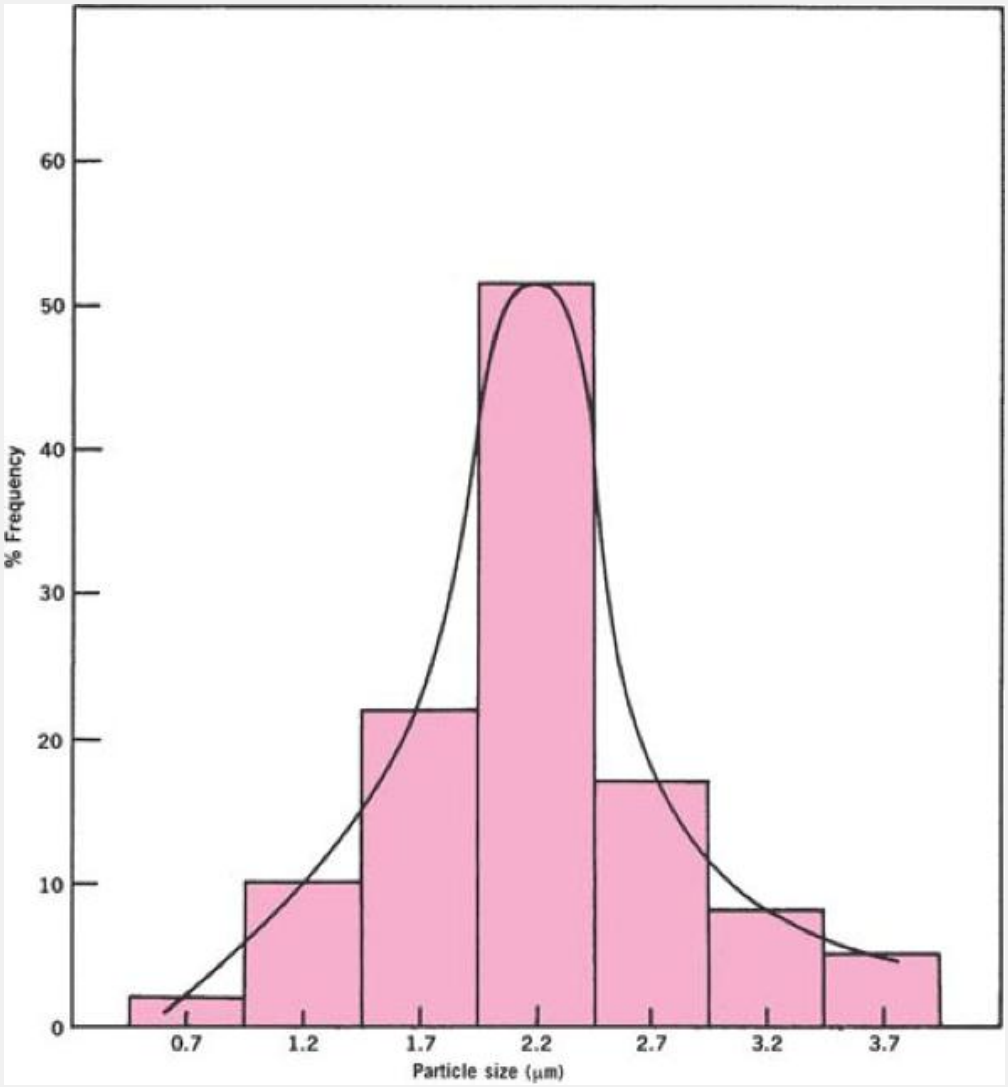

Fig. 18-1. A plot of the data of Table 18-4 so as to yield a size–frequency distribution. The data are plotted as a bar graph or *histogram*, and a superimposed smooth line or frequency curve is shown drawn through the histogram.

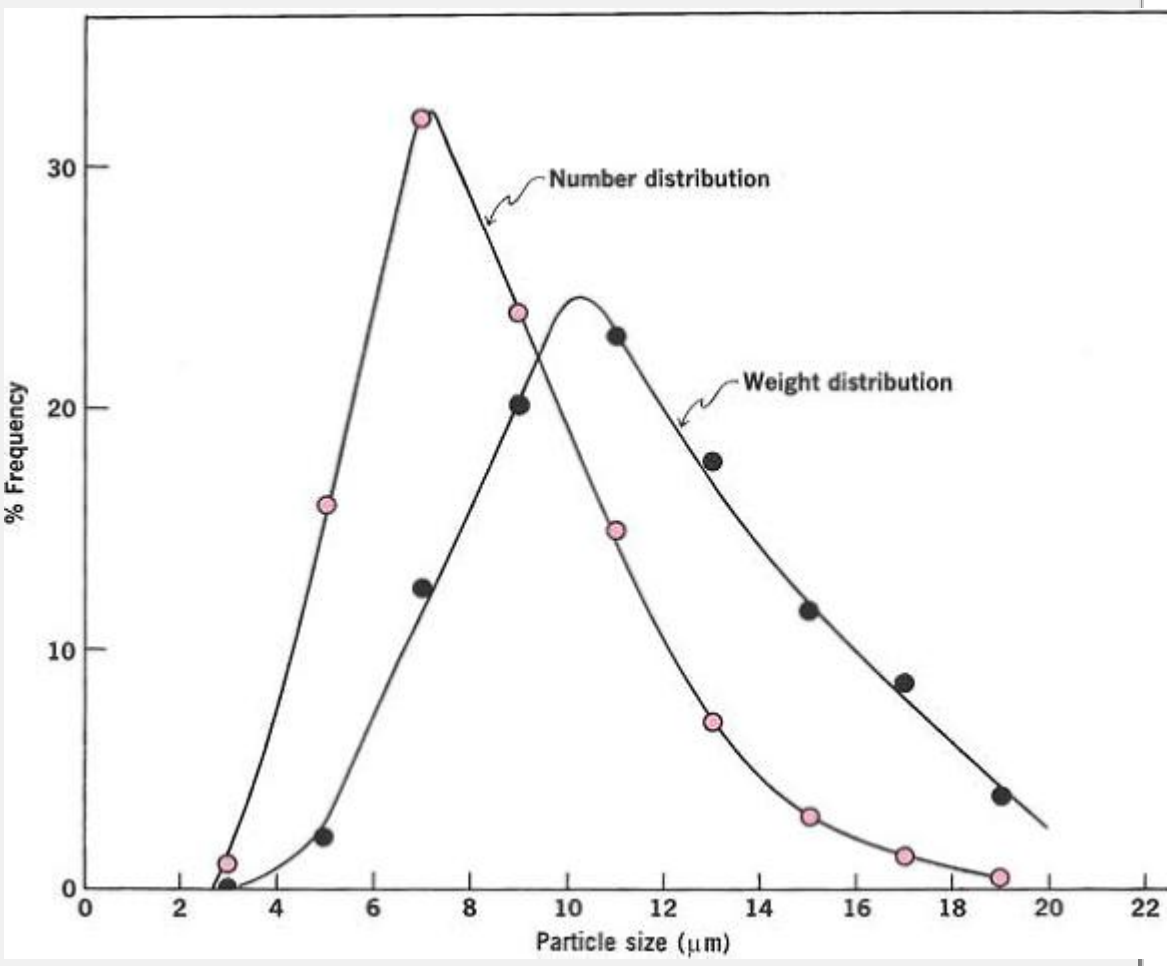

Fig. 18-2. Frequency distribution plot of the data in Table 18-6.

Table 18-6 Conversion of Number Distribution to Weight Distribution (Log-Normal Distribution)

(1) Size Range (μm)	(2) Mean of Size Range, d (μm)	(3) Number of Particles in Each Size Range, n	(4) Percent, n	(5) Cumulative Percent Frequency Undersize (Number)	(6) nd	(7) nd^2	(8) nd^3	(9) Percent nd^3 (Weight)	(10) Cumulative Percent Frequency Undersize (Weight)
2.0–4.	3.0	2	1.0	1.0	6	18	54	0.03	0.03

0									
4.0–6.0	5.0	32	16.0	17.0	160	800	4000	2.31	2.34
6.0–8.0	7.0	64	32.0	49.0	448	3136	21952	12.65	14.99
8.0–10.0	9.0	48	24.0	73.0	432	3888	34992	20.16	35.15
10.0–12.0	11.0	30	15.0	88.0	330	3630	39930	23.01	58.16
12.0–14.0	13.0	14	7.0	95.0	182	2366	30758	17.72	75.88
14.0–16.0	15.0	6	3.0	98.0	90	1350	20250	11.67	87.55
16.0–18.0	17.0	3	1.5	99.5	51	867	14739	8.49	96.04

18.0–20.0	19.0	1	0.5	100.0	19	361	6859	3.95	99.99
		$\sum n = 200$							

The reader should be familiar with the concept of a *normal*distribution. As the name implies, the distribution is symmetric around the mean, which is also the mode.

The standard deviation, σ, is an indication of the distribution about the mean.* In a normal distribution, 68% of the population lies ±1 $\sigma$from the mean, 95.5% lies within the mean ±2 σ, and 99.7% lies within the mean ±3 σ. The normal distribution, shown in Figure 18-1, is not commonly found in pharmaceutical powders, which are frequently processed by milling or precipitation.6 Rather, these systems tend to have an nonsymmetric, or skewed, distribution of the type depicted in Figure 18-2. When the data in Figure 18-2 (taken from Table 18-6) are plotted as frequency versus the *logarithm* of the particle diameter, a typical bell-shaped curve is frequently obtained. This is depicted in Figure 18-4. A size distribution fitting this pattern is spoken of as a *log-normal distribution*, in contrast to the normal distribution shown in Figure 18-1.

A log-normal distribution has several properties of interest. When the logarithm of the particle size is plotted against the cumulative percent frequency on a probability scale, a linear relationship is observed (Fig. 18-5). Such a linear plot has the distinct advantage that we can now characterize a log-normal distribution *curve* by means of two parameters—the slope of the line and a reference point. Knowing these two parameters, we can reproduce Figure 18-5and, by working back, can come up with a good approximation ofFigure 18-2, Figure 18-3, or Figure 18-4. The reference point used is the logarithm of the particle size equivalent to 50% on the probability scale, that is, the 50% size. This is known as the *geometric mean diameter* and is given the symbol d_g. The slope is given by the geometric standard deviation, σ_g, which is the quotient of the ratio (84% undersize or 16% oversize)/(50% size) or (50% size)/(16% undersize or 84% oversize). This is simply the slope of the straight line. In Figure 18-5, for the number distribution data, d_g = 7.1 μm andσ_g = 1.43. Sano et al.7 used a spherical agglomeration technique with soluble polymers and surfactants to increase the dissolution rate of the poorly soluble crystals of tolbutamide. The spherical particles were free flowing and yielded log probability plots as shown in Figure 18-5. The dissolution of the tolbutamide agglomerates followed the Hixon–Crowell cube root equation, as did the dissolution rate of tolbutamide crystals alone.

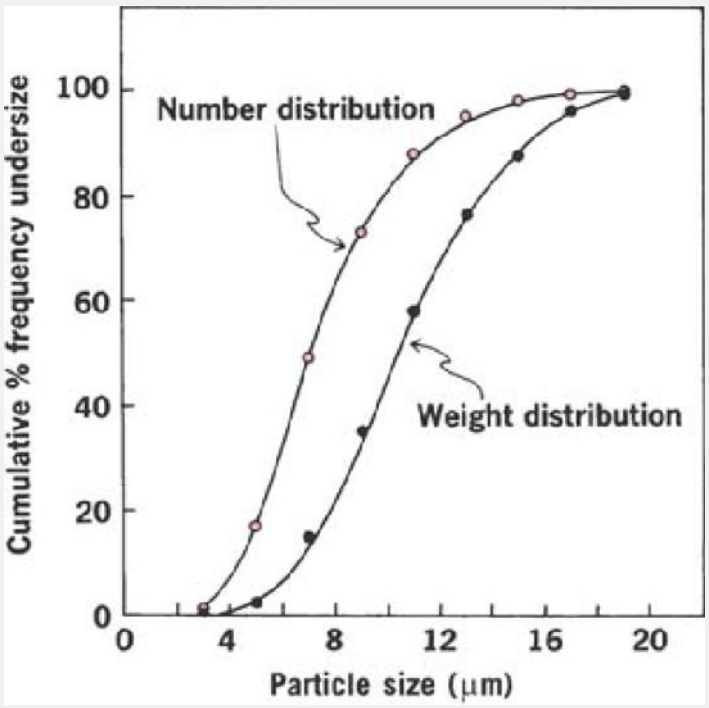

Fig. 18-3. Cumulative frequency plot of the data inTable 18-6.

P.448

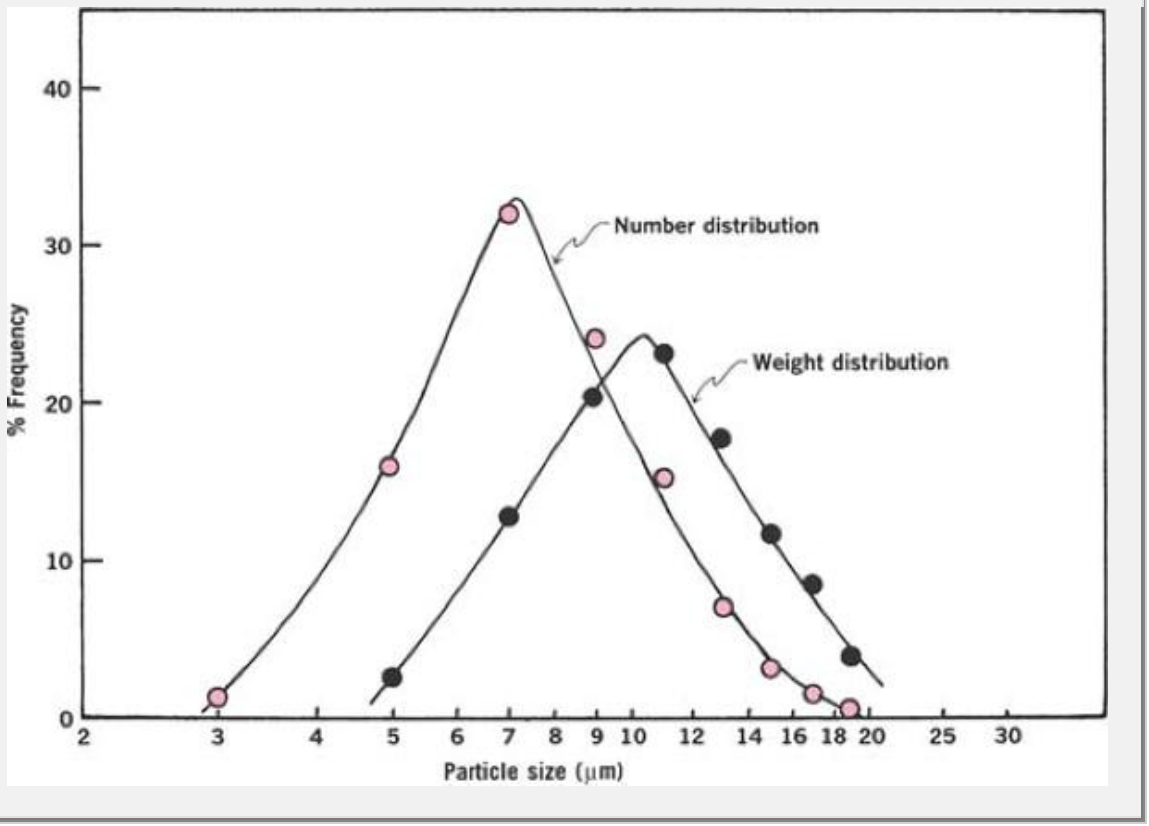

Fig. 18-4. Frequency distribution plot of the data in Table 18-6 showing log-normal relation.

Number and Weight Distributions

The data in Table 18-6 are shown as a number distribution, implying that they were collected by a counting technique such as microscopy. Frequently, we are interested in obtaining data based on a weight, rather than a number, distribution. Although this can be achieved by using a technique such as sedimentation or sieving, it will be more convenient, if the number data are already at hand, to convert the number distribution to a weight distribution and vice versa.

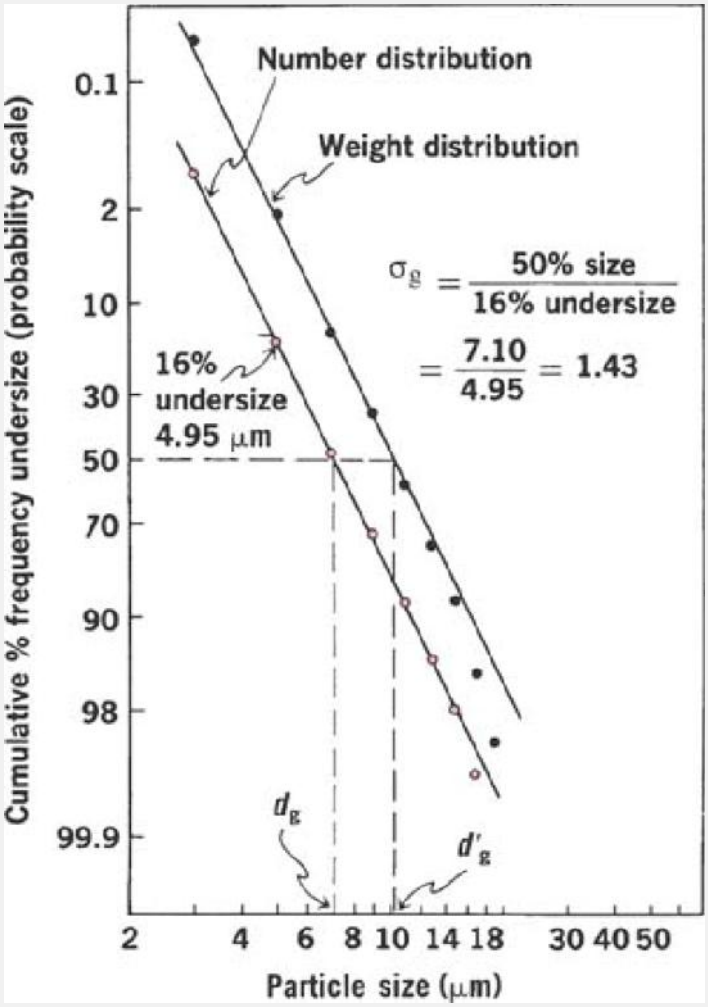

Fig. 18-5. Log probability plots of the data in Table 18-6.

Two approaches are available. Provided the general shape and density of the particles are independent of the size range present in the sample, an estimate of the weight distribution of the data inTable 18-6 can be obtained by calculating the values shown in columns 9 and 10. These are based on nd^3 in column 8. These data have been plotted alongside the number distribution data in Figures 18-2 and 18-3, respectively.

The significant differences in the two distributions are apparent, even though they relate to the same sample. For example, in Figure 18-3, only 12% of the sample by number is greater than 11 μm, yet these same particles account for 42% of the total weight of the particles. For this reason, it is important

to distinguish carefully between size distributions on a weight and a number basis. Weight distributions can also be plotted in the same manner as the number distribution data, as seen in Figures 18-4 and 18-5. Note that inFigure 18-5 the slope of the line for the weight distribution is identical with that for the number distribution. Thus, the geometric standard deviation on a weight basis, σ'_g, also equals 1.43. Customarily, the prime is dropped because the value is independent of the type of distribution. The geometric mean diameter (the particle size at the 50% probability level) on a weight basis, d'_g, is 10.4 μm, whereas d_g = 7.1 μm.

Provided the distribution is log-normal, the second approach is to use one of the equations developed by Hatch

and Choate.8 By this means, it is possible to convert number distributions to weight distributions with a minimum of calculation. In addition, a particular average can be readily computed by use of the relevant equation. The Hatch–Choate equations are listed in Table 18-7.

Table 18-7 Hatch–Choate Equations for Computing Statistical Diameters from Number and Weight Distributions

Diameter	Number Distribution	Weight Distribution
Length-number mean	$\log d_{ln} = \log d_g + 1.151 \log^2 \sigma_g$	$\log d_{ln} = \log d_g' - 5.757 \log^2 \sigma_g$
Surface-number mean	$\log d_{sn} = \log d_g + 2.303 \log^2 \sigma_g$	$\log d_{sn} = \log d_g' - 4.606 \log^2 \sigma_g$
Volume-number mean	$\log d_{vn} = \log d_g + 3.454 \log^2 \sigma_g$	$\log d_{vn} = \log d_g' - 3.454 \log^2 \sigma_g$
Volume-surface mean	$\log d_{vs} = \log d_g + 5.757 \log^2 \sigma_g$	$\log d_{vs} = \log d_g' - 1.151 \log^2 \sigma_g$
Weight-moment mean	$\log d_{wm} = \log d_g + 8.059 \log^2 \sigma_g$	$\log d_{wm} = \log d_g' + 1.151 \log^2 \sigma_g$

Example 18-1
Using Distribution Data

From the number distribution data in Table 18-6 and Figure 18-5, it is found that d_g = 7.1 μm and σ_g = 1.43, or log σ_g = 0.1553. Using the relevant Hatch–Choate equation, calculate d_{ln} and d'_g.

The equation for the length-number mean, d_{ln}, is

$$\begin{aligned} \log d_{ln} &= \log d_g + 1.151 \log^2 \sigma_g \\ &= 0.8513 + 1.151(0.1553)^2 \\ &= 0.8513 + 0.0278 \\ &= 0.8791 \\ d_{ln} &= 7.57\ \mu m \end{aligned}$$

To calculate d'_g, we must substitute into the following Hatch–Choate equation:

$$\log d_{\ln} = \log d'_g - 5.757 \log^2 \sigma_g$$
$$8.791 = \log d'_g - 5.757(0.1553)^2$$

or

$$\log d'_g = 0.8791 + 0.1388$$
$$= 1.0179$$
$$d'_g = 10.4\,\mu\text{m}$$

One can also use an equation suggested by Rao,9

$$d'_g = d_g \sigma_g^{(3 \ln \sigma_g)} \qquad (18\text{–}2)$$

to readily obtain d'_g knowing d_g and σ_g. In this example,

$$d'_g = 7.1(1.43)^{(3 \ln 1.43)}$$
$$= 10.42$$

The student should confirm that substitution of the relevant data into the remaining Hatch–Choate equations in Table 18-7 yields the following statistical diameters:

$$d_{sn} = 8.07\,\mu\text{m}; \quad d_{vn} = 8.60\,\mu\text{m};$$
$$d_{vs} = 9.78\,\mu\text{m}; \quad d_{wm} = 11.11\,\mu\text{m}$$

Particle Number

A significant expression in particle technology is the *number of particles per unit weight, N*, which is expressed in terms of d_{vn}.

The number of particles per unit weight is obtained as follows. Assume that the particles are spheres, the volume of a single particle is $\pi d3_{vn}/6$, and the mass (volume × density) is $(\pi d_{vn}3\rho)/6$ g per particle. The number of particles per gram is then obtained from the proportion

$$\frac{(\pi d_{vn}^3 \rho)/6 \text{ g}}{1 \text{ particle}} = \frac{1 \text{ g}}{N} \qquad (18\text{–}3)$$

and

$$N = \frac{6}{\pi d_{vn}^3 \rho} \qquad (18\text{–}4)$$

Example 18-2
Number of Particles

The mean volume number diameter of the powder, the data for which are given in Table 18-4, is 2.41 μm, or 2.41×10^{-4}cm. If the density of the powder is 3.0 g/cm^3, what is the number of particles per gram?

We have

$$N = \frac{6}{3.14 \times (2.41 \times 10^{-4})^3 \times 3.0} = 4.55 \times 10^{10}$$

Methods for Determining Particle Size

Many methods are available for determining particle size. Only those that are widely used in pharmaceutical practice and are typical of a particular principle are presented. For a detailed discussion of the numerous methods of particle size analysis, consult the work by Edmundson5 and Allen10 and the references given there to other sources. The methods available for determining the size characteristics of submicrometer particles were reviewed by Groves.11

Microscopy, sieving, sedimentation, and the determination of particle volume are discussed in the following section. None of the measurements are truly direct methods. Although the microscope allows the observer to view the actual particles, the results obtained are probably no more “direct” than those resulting from other methods because only two of the three particle dimensions are ordinarily seen. The sedimentation methods yield a particle size relative to the rate at which particles settle through a suspending medium, a measurement important in the development of emulsions and suspensions. The measurement of particle volume, using an

apparatus called the Coulter counter, allows one to calculate an equivalent volume diameter.

However, the technique gives no information as to the shape of the particles. Thus, in all these cases, the size may or may not compare with that obtained by the microscope or by other methods; the size is most directly applicable to the analysis for which it is intended. A guide to the range of particle sizes applicable to each method is given in Figure 18-6.

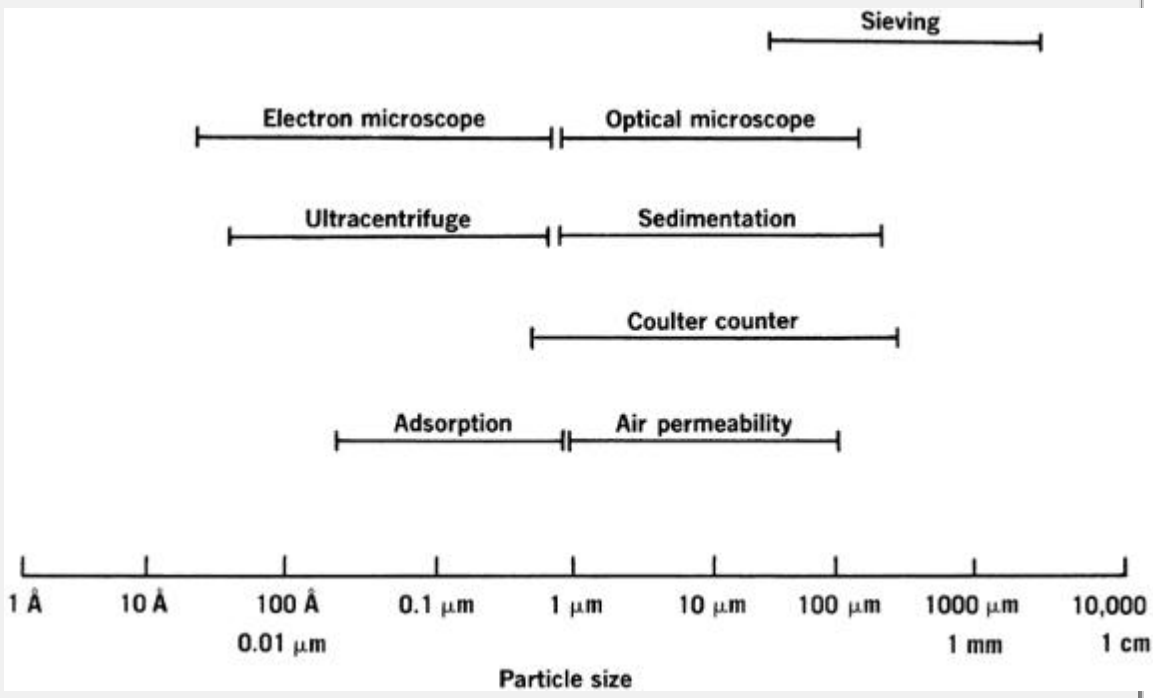

Fig. 18-6. Approximate size ranges of methods used for particle-size and specific-surface analysis.

Optical Microscopy

It should be possible to use the ordinary microscope for particle-size measurement in the range of 0.2 to about 100 μm. According to the microscopic method, an emulsion or suspension, diluted or undiluted, is mounted on a slide or ruled cell and placed on a mechanical stage. The microscope eyepiece is fitted with a micrometer by which the size of the particles can be estimated. The field can be projected onto a screen where the particles are measured more easily, or a photograph can be taken from which a slide is prepared and projected on a screen for measurement.

The particles are measured along an arbitrarily chosen fixed line, generally made horizontally across the center of the particle. Popular measurements are the *Feret diameter*, the *Martin diameter*,12 and the *projected area diameter*, all of which can be defined by reference to Figure 18-7, as suggested by Allen.13 Martin's diameter is the length of a line that bisects the particle image. The line can be drawn in any direction but must be in the same direction for all particles measured. The Martin diameter is identified by the number 1 inFigure 18-7. Feret's diameter, corresponding to the number 2 in the figure, is the distance between two tangents on opposite sides of the particle parallel to some fixed direction, the *y* direction in the figure. The third measurement, number 3 in Figure 18-7, is the projected area diameter. It is the diameter of a circle with the same area as that of the particle observed perpendicular to the surface on which the particle rests.

A size–frequency distribution curve can be plotted as in Figure 18-1for the determination of the statistical diameters of the distribution. Electronic scanners have been developed to remove the necessity of measuring the particles by visual observation.

Prasad and Wan14 used video recording equipment to observe, record, store, and retrieve particle-size data from a microscopic examination of tablet excipients, including microcrystalline cellulose, sodium

carboxymethylcellulose, sodium starch glycolate, and methylcellulose. The projected area of the particle profile, Feret's diameter, and various shape factors (elongation, bulkiness, and surface factor) were

determined. The video recording technique was found to be simple and convenient for microscopic examination of excipients.

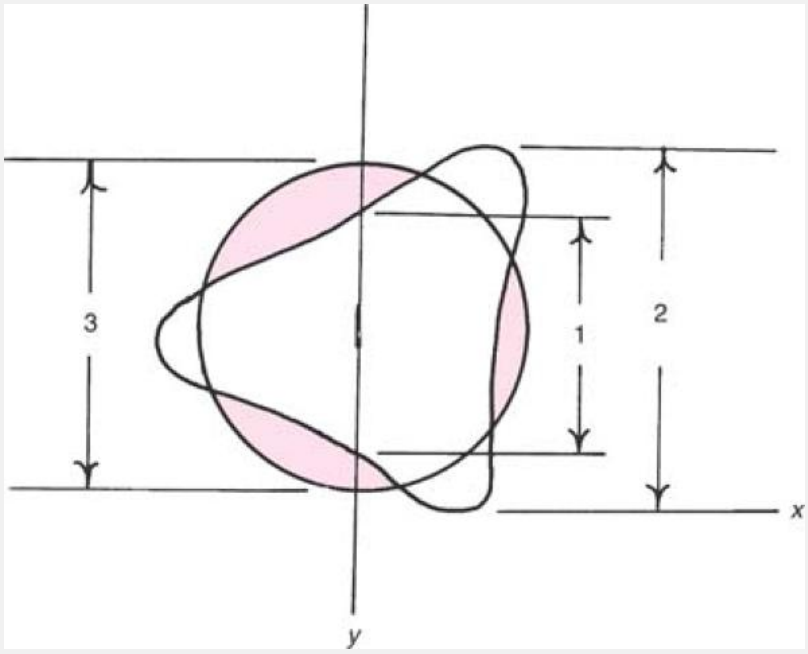

Fig. 18-7. A general diagram providing definitions of the Feret, Martin, and projected diameters. (From T. Allen,*Particle Size Measurements*, 2nd Ed., Chapman Hall, London, 1974, p. 131. With permission.)

A disadvantage of the microscopic method is that the diameter is obtained from only two dimensions of the particle: length and breadth. No estimation of the depth (thickness) of the particle is ordinarily available. In addition, the number of particles that must be counted (300–500) to obtain a good estimation of the distribution makes the method somewhat slow and tedious. Nonetheless, microscopic examination (photomicrographs) of a sample should be undertaken even when other methods of particle-size analysis are being used, because the presence of agglomerates and particles of more than one component may often be detected.

Sieving

This method uses a series of standard sieves calibrated by the National Bureau of Standards. Sieves are generally used for grading coarser particles; if extreme care is used, however, they can be employed for screening material as fine as 44 μm (No. 325 sieve). Sieves produced by photoetching and electroforming techniques are available with apertures from 90 μm to as low as 5 μm. According to the method of the *U. S. Pharmacopeia* for testing powder fineness, a mass of sample is placed on the proper sieve in a mechanical shaker. The powder is shaken for a definite period of time, and the material that passes through one sieve and is retained on the next finer sieve is collected and weighed. Another approach is to assign the particles on the lower sieve with the arithmetic or geometric mean size of the two screens. Arambulo and Deardorff15 used this method of size classification in their analysis of the average weight of compressed tablets. Frequently the powder is assigned the mesh number of the screen through which it passes or on which it is retained. King and Becker16 expressed the size ranges of calamine samples in this way in their study of calamine lotion.

When a detailed analysis is desired, the sieves can be arranged in a nest of about five with the coarsest at the top. A carefully weighed sample of the powder is placed on the top sieve, and after the sieves are shaken for a predetermined period of time, the powder retained on each sieve is weighed. Assuming a log-normal distribution, one plots the cumulative percent by weight of powder retained on the sieves on the probability scale against the logarithm of the arithmetic mean size of the openings of each of two successive screens. As illustrated in Figure 18-5, the geometric mean weight diameter, d'_g, and the geometric standard deviation, σ_g, can be obtained directly from the straight line.

According to Herdan,17 sieving errors can arise from a number of variables including sieve loading and duration and intensity of agitation. Fonner et al.18 demonstrated that sieving can cause attrition of granular pharmaceutical materials. Care must be taken, therefore, to ensure that reproducible techniques are employed so that different particle-size distributions between batches of material are not due simply to different sieving conditions.

Sedimentation

The application of ultracentrifugation to the determination of the molecular weight of high polymers has already been discussed. The particle size in the subsieve range can be obtained by gravity sedimentation as expressed in Stokes's law,

$$v = \frac{h}{t} = \frac{d_{st}^2(\rho_s - \rho_0)g}{18\eta_0} \qquad (18\text{–}5)$$

or

$$d_{st} = \sqrt{\frac{18\eta_0 h}{(\rho_s - \rho_0)gt}} \qquad (18\text{–}6)$$

where v is the rate of settling, h is the distance of fall in time t, d_{st} is the mean diameter of the particles based on the velocity of sedimentation, ρ_s is the density of the particles and ρ_0 that of the dispersion medium, g is the acceleration due to gravity, and η_0 is the viscosity of the medium. The equation holds exactly only for spheres falling freely without hindrance and at a constant rate. The law is applicable to irregularly shaped particles of various sizes as long as one realizes that the diameter obtained is a relative particle size equivalent to that of sphere falling at the same velocity as that of the particles under consideration. The particles must not be aggregated or clumped together in the suspension because such clumps would fall more rapidly than the individual particles and erroneous results would be obtained. The proper deflocculating agent must be found for each sample that will keep the particles free and separate as they fall through the medium.

Example 18-3

Stokes Diameter

A sample of powdered zinc oxide, density 5.60 g/cm^3, is allowed to settle under the acceleration of gravity, 981 cm/sec^2, at 25°C. The rate of settling, v, is 7.30 × 10^{-3}cm/sec; the density of the medium is 1.01 g/cm^3, and its viscosity is 1 centipoise = 0.01 poise or 0.01 g/cm sec. Calculate the Stokes diameter of the zinc oxide powder.

We have

$$d_{st} = \sqrt{\frac{(18 \times 0.01 \text{ g/cm sec}) \times (7.30 \times 10^{-3} \text{ cm/sec})}{(5.60 - 1.01 \text{ g/cm}^3) \times (981 \text{ cm/sec}^2)}}$$

$$= 5.40 \times 10^{-4} \text{ cm or } 5.40\ \mu\text{m}$$

For Stokes's law to apply, a further requirement is that the flow of dispersion medium around the particle as it sediments is *laminar* or*streamline*. In other words, the rate of sedimentation of a particle must not be so rapid that turbulence is set up, because this in turn will affect the sedimentation of the particle. Whether the flow is turbulent or laminar is indicated by the dimensionless *Reynolds number*, R_e, which is defined as

$$R_e = \frac{v\, d\rho_0}{\eta_0} \qquad (18\text{–}7)$$

where the symbols have the same meaning as in equation (18-5). According to Heywood,19 Stokes's law cannot be used if

R_e is greater than 0.2 because turbulence appears at this value. On this basis, the limiting particle size under a given set of conditions can be calculated as follows.

Rearranging equation (18-7) and combining it with equation (18-5)gives

$$v = \frac{R_e \eta}{d\rho_0} = \frac{d^2(\rho_s - \rho_0)g}{18\eta} \qquad (18\text{–}8)$$

and thus

$$d^3 = \frac{18R_e\eta^2}{(\rho_s - \rho_0)\rho_0 g} \qquad (18\text{–}9)$$

Under a given set of density and viscosity conditions, equation (18-9)allows calculation of the maximum particle diameter whose sedimentation will be governed by Stokes's law, that is, when $R_e$does not exceed 0.2.

Example 18-4

Largest Particle Size

A powdered material, density 2.7 g/cm^3, is suspended in water at 20°C. What is the size of the largest particle that will settle without causing turbulence? The viscosity of water at 20°C is 0.01 poise, or g/cm sec, and the density is 1.0 g/cm^3.

From equation (18-9),

$$d^3 = \frac{(18)(0.2)(0.01)^2}{(2.7 - 1.0)1.0 \times 981}$$

$$d = 6 \times 10^{-3}\ \text{cm} = 60\ \mu\text{m}$$

Example 18-5

Particle Size, Setting, and Viscosity

If the material used in Example 18-4 is now suspended in a syrup containing 60% by weight of sucrose, what will be the critical diameter, that is, the maximum diameter for whichR_e does not exceed 0.2? The viscosity of the syrup is 0.567 poise, and the density is 1.3 g/cm^3.

We have

$$d^3 = \frac{(18)(0.2)(0.567)^2}{(2.7 - 1.3)1.3 \times 981}$$

$$d = 8.65 \times 10^{-2}\ \text{cm} = 865\ \mu\text{m}$$

Several methods based on sedimentation are used. Principal among these are the pipette method, the balance method, and the hydrometer method. Only the first technique is discussed here because it combines ease of analysis, accuracy, and economy of equipment.

The Andreasen apparatus is shown in Figure 18-8. It usually consists of a 550 mL vessel containing a 10 mL pipette sealed into a ground-glass stopper. When the pipette is in place in the cylinder, its lower tip is 20 cm below the surface of the suspension.

The analysis is carried out in the following manner. A 1% or 2% suspension of the particles in a medium containing a suitable deflocculating agent is introduced into the vessel and brought to the 550 mL mark. The stoppered vessel is shaken to distribute the particles uniformly throughout the suspension, and the apparatus, with pipette in place, is clamped securely in a constant-temperature bath. At various time intervals, 10 mL samples are withdrawn and discharged by means of the two-way stopcock. The samples are evaporated and weighed or analyzed by other appropriate means, correcting for the deflocculating agent that has been added.

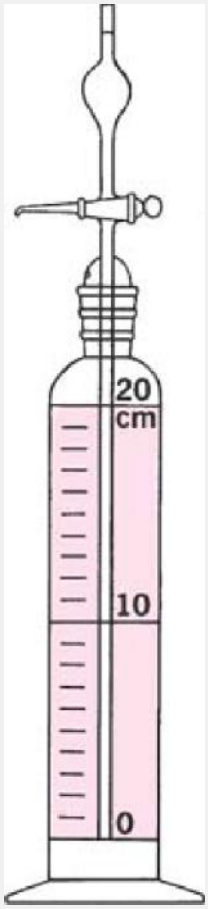

Fig. 18-8. Andreasen apparatus for determining particle size by the gravity sedimentation method.

The particle diameter corresponding to the various time periods is calculated from Stokes's law, with *h* in equation **(**18-6**)** being the height of the liquid above the lower end of the pipette at the time each sample is removed. The residue or dried sample obtained at a particular time is the weight fraction having particles of sizes less than the size obtained by the Stokes-law calculation for that time period of settling. The weight of each sample residue is therefore called the *weight undersize*, and the sum of the successive weights is known as the *cumulative weight undersize*. It can be expressed directly in weight units or as percentage of the total weight of the final sediment. Such data are plotted in Figures 18-2, 18-3 and 18-4. The cumulative percentage by weight undersize can then be plotted on a probability scale against the particle diameter on a log scale, as inFigure 18-5, and the statistical diameters obtained as explained previously.

Particle Volume Measurement

A popular instrument for measuring the volume of particles is the Coulter counter (Fig. 18-9). This instrument operates on the principle that when a particle suspended in a conducting liquid passes through a small orifice on either side of which are electrodes, a change in electric resistance occurs. In practice, a known volume of a dilute suspension is pumped through the orifice. Provided the suspension is sufficiently dilute, the particles pass through essentially one at a time. A constant voltage is applied across the electrodes to produce a current. As the particle travels through the orifice, it

displaces its own volume of electrolyte, and this results in an increased resistance between the two

electrodes. The change in resistance, which is related to the particle volume, causes a voltage pulse that is amplified and fed to a pulse-height analyzer calibrated in terms of particle size. The instrument records electronically all those particles producing pulses that are within two threshold values of the analyzer. By systematically varying the threshold settings and counting the number of particles in a constant sample size, it is possible to obtain a particle-size distribution. The instrument is capable of counting particles at the rate of approximately 4000 per second, and so both gross counts and particle-size distributions are obtained in a relatively short period of time. The data may be readily converted from a volume distribution to a weight distribution.

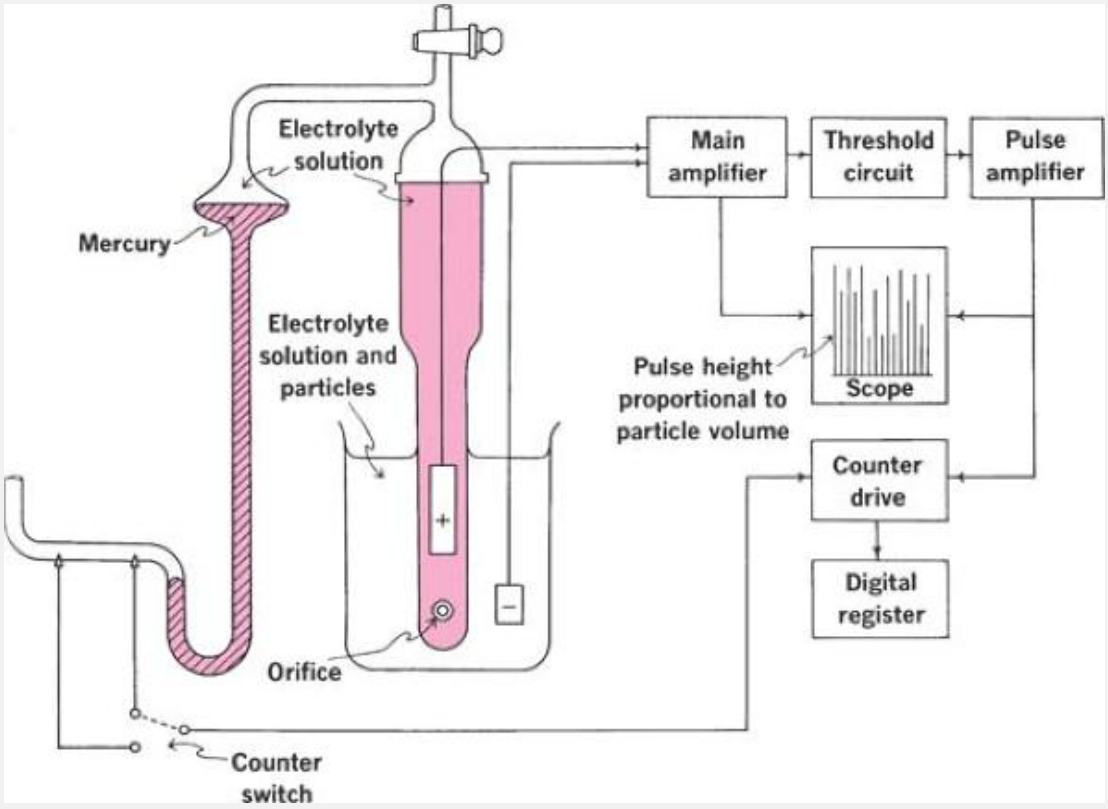

Fig. 18-9. Schematic diagram of a Coulter counter, used to determine particle volume.

The Coulter counter has been used to advantage in the pharmaceutical sciences to study particle growth and dissolution[20,21] and the effect of antibacterial agents on the growth of microorganisms.[22] The use of the Coulter particle-size analyzer together with a digital computer was reported by Beaubien and Vanderwielen[23] for the automated particle counting of milled and micronized drugs. Samples of spectinomycin hydrochloride and a micronized steroid were subjected to particle-size analysis together with polystyrene spheres of 2.0 to 80.0 μm diameter, which were used to calibrate the apparatus. The powders showed log-normal distributions and were well characterized by geometric volume mean diameters and geometric standard deviations. Accurate particle sizes were obtained between 2 and 80 μm diameter with a precision of about 0.5 μm. The authors concluded that the automated Coulter counter was quite satisfactory for quality control of pharmaceutical powders. The Coulter particle counter was used by Ismail and Tawashi[24] to obtain size distributions of the mineral part of human kidney (urinary) stones and to determine whether there is a critical size range for stone formation. The study provided a better understanding of the clustering process and the packing of the mineral components of renal stones.

Beckman Coulter also manufactures a *submicron*-particle sizing instrument, the Beckman Coulter Model N5, for analyzing particles in the size range of 0.0033 to 0.3 μm. By the use of photon correlation

spectroscopy, the instrument senses the Brownian motion of the particles in suspension. The smaller a particle, the faster it moves by Brownian motion. A laser beam passes through the sample and a sensor detects the light scattered by the particles undergoing Brownian motion. The Beckman Coulter Model N5 instrument provides not only particle-size and size distribution data but also molecular weights and diffusion coefficients. Submicron size determination is important in pharmacy in the analysis of microemulsions, pigments and dyes, colloids, micelles and solubilized systems, liposomes, and microparticles.

An investigation of contaminant particulate matter in parenteral solutions for adherence to the standards set by the 1986 Italian*Pharmacopóeia* was conducted by Signoretti et al.25 They studied the number and nature of the particulates in 36 large-volume injectable solutions using scanning electron microscopy and x-ray analysis. About one fifth of the samples showed a considerable number of particles of sizes greater than 20 μm in diameter. The particles were identified as textile fibers, cellulose, plastic material, and contaminants from the manufacturing and packaging processes, such as pieces of rubber and bits of metal. Because of their number, size, shape, surface properties, and chemical nature, these contaminants can cause vascular occlusions and inflammatory, neoplastic, and allergic reactions. Embolisms may occur with particles larger than 5 μm.

According to the standards of the Italian *Pharmacopóeia* for parenteral solutions of greater than 100 mL, no more than 100 particles 5 μm and larger and no more than four particles 20 μm in diameter and larger may be present in each milliliter of solution. These workers found that a considerable number of the manufacturers failed to produce parenteral preparations within the limits of the Pharmacopóeia, the contaminants probably occurring in most cases from filters, clothing, and container seals.

In the preparation of indomethacin sustained-release pellets, Li et al.26 used a Microtrac particle-size analyzer (Leeds and Northrup Instruments) to determine the particle size of indomethacin as obtained from the manufacturer and as two types of micronized powder. The powders were also examined under a microscope with a magnification of 400×, and photomicrographs were taken with a Polaroid SX-70 camera. Pellets (referred to as IS pellets) containing indomethacin and Eudragit S-100 were prepared using a fluid bed granulator or a Wurster column apparatus. Eudragit (Röhm Pharma) is an acrylic polymer for the enteric coating of tablets, capsules, and pellets. Its surface properties and chemical structure as a film coating polymer were reviewed by Davies et al.27 Sieve analysis with U.S. standard sieves Nos. 12, 14, 16, 18, 20, 25, and 35 was used to determine the particle-size distribution of the IS pellets. The yield of IS pellets depended greatly on the particle size of the indomethacin powder. Batches using two micronized powders (average diameter of 3.3 and 6.4 μm, respectively) produced a higher yield of the IS pellets than did the original indomethacin powder (40.6 μm) obtained directly from the drug manufacturer. Davies et al.27 concluded that both the average particle diameter and the particle-size distribution of the indomethacin powder must be considered for maximum yield of the sustained-release pellets.

Carli and Motta28 investigated the use of microcomputerized mercury porosimetry to obtain particle-size and surface area distributions of pharmaceutical powders. Mercury porosimetry gives the volume of the pores of a powder, which is penetrated by mercury at each successive pressure; the pore volume is converted into a pore-size distribution. The total surface area and particle size of the powder can also be obtained from the mercury porosimetry data.

Particle Shape and Surface Area

Knowledge of the shape and the surface area of a particle is desirable. The shape affects the flow and packing properties of a powder as well as having some influence on the surface area. The surface area per unit weight or volume is an important characteristic of a powder when one is undertaking surface adsorption and dissolution rate studies.

Particle Shape

A sphere has minimum surface area per unit volume. The more asymmetric a particle, the greater is the surface area per unit volume. As discussed previously, a spherical particle is characterized completely by its diameter. As the particle becomes more asymmetric, it becomes increasingly difficult to assign a meaningful diameter to the particle—hence, as we have seen, the need for equivalent spherical diameters. It is a simple matter to obtain the surface area or volume of a sphere because for such a particle

$$\text{Surface area} = \pi d^2 \qquad (18\text{–}10)$$

and

$$\text{Volume} = \frac{\pi d^3}{6} \qquad (18\text{–}11)$$

where d is the diameter of the particle. The surface area and volume of a spherical particle are therefore proportional to the square and cube, respectively, of the diameter. To obtain an estimate of the surface or volume of a particle (or collection of particles) whose shape is not spherical, however, one must choose a diameter that is characteristic of the particle and relate this to the surface area or volume through a correction factor. Suppose the particles are viewed microscopically, and it is desired to compute the surface area and volume from the projected diameter, d_p, of the particles. The square and cube of the chosen dimension (in this case, d_p) are proportional to the surface area and volume, respectively. By means of proportionality constants, we can then write

$$\text{Surface area} = \alpha_s d_p^2 = \pi d_s^2 \qquad (18\text{–}12)$$

where α_s is the surface area factor and d_s is the equivalent surface diameter. For volume we write

$$\text{Volume} = \alpha_v d_p^3 = \frac{\pi d_v^2}{6} \qquad (18\text{–}13)$$

where α_v is the volume factor and d_v is the equivalent volume diameter. The surface area and volume "shape factors" are, in reality, the ratio of one diameter to another. Thus, for a sphere, $\alpha_s = \pi d_s 2/d_p 2 = 3.142$ and $\alpha_v = \pi d_v 3/6\, d_p 3 = 0.524$. There are as many of these volume and shape factors as there are pairs of equivalent diameters. The ratio α_s/α_v is also used to characterize particle shape. When the particle is spherical, $\alpha_s/\alpha_v = 6.0$. The more asymmetric the particle, the more this ratio exceeds the minimum value of 6.

Specific Surface

The specific surface is the surface area per unit volume, S_v, or per unit weight, S_w, and can be derived from equations (18-12) and (18-13). Taking the general case, for asymmetric particles where the characteristic dimension is not yet defined,

$$S_v = \frac{\text{Surface area of particles}}{\text{Volume of particles}}$$

$$= \frac{n\alpha_s d^2}{n\alpha_v d^3} = \frac{\alpha_s}{\alpha_v d} \qquad (18\text{–}14)$$

where n is the number of particles. The surface area per unit weight is therefore

$$S_w = \frac{S_v}{\rho} \qquad (18\text{–}15)$$

where ρ is the true density of the particles. Substituting for equation (18-14) in (18-15) leads to the general equation

$$S_w = \frac{\alpha_s}{\rho d_{vs} \alpha_v} \qquad (18\text{–}16)$$

where the dimension is now defined as d_{vs}, the volume–surface diameter characteristic of specific surface. When the particles are spherical (or nearly so), equation (18-16) simplifies to

$$S_w = \frac{6}{\rho d_{vs}} \qquad (18\text{–}17)$$

because $\alpha_s/\alpha_v = 6.0$ for a sphere.

Example 18-6
Surface Area
What are the specific surfaces, S_w and S_v, of particles assumed to be spherical in which ρ = 3.0 g/cm^3 and $d_{vs}$from Table 18-5 is 2.57 μm?
We have

$$S_w = \frac{6}{3.0 \times 2.57 \times 10^{-4}} = 7.78 \times 10^3 \text{ cm}^2/\text{g}$$

$$S_v = \frac{6}{2.57 \times 10^{-4}} = 2.33 \times 10^4 \text{ cm}^2/\text{cm}^3$$

Methods for Determining Surface Area

The surface area of a powder sample can be computed from knowledge of the particle-size distribution obtained using one of the methods outlined previously. Two methods are commonly available that permit direct calculation of surface area. In the first, the amount of a gas or liquid solute that is *adsorbed* onto the sample of powder to form a monolayer is a direct function of the surface area of the sample. The second method depends on the fact that the rate at which a gas or liquid *permeates* a bed of powder is related, among other factors, to the surface area exposed to the permeant.

Adsorption Method

Particles with a large specific surface are good adsorbents for the adsorption of gases and of solutes from solution. In determining the surface of the adsorbent, the volume in cubic centimeters of gas adsorbed per gram of adsorbent can be plotted against the pressure of the gas at constant temperature to give a type II *isotherm*as shown in Figure 18-10.
The adsorbed layer is monomolecular at low pressures and becomes multimolecular at higher pressures. The completion of the monolayer of nitrogen on a powder is shown as point *B* in Figure 18-10. The volume of nitrogen gas, V_m, in cm^3 that 1 g of the powder can adsorb when the monolayer is complete is more accurately given by using the Brunaver, Emmett, and Teller (BET) equation, which can be written as

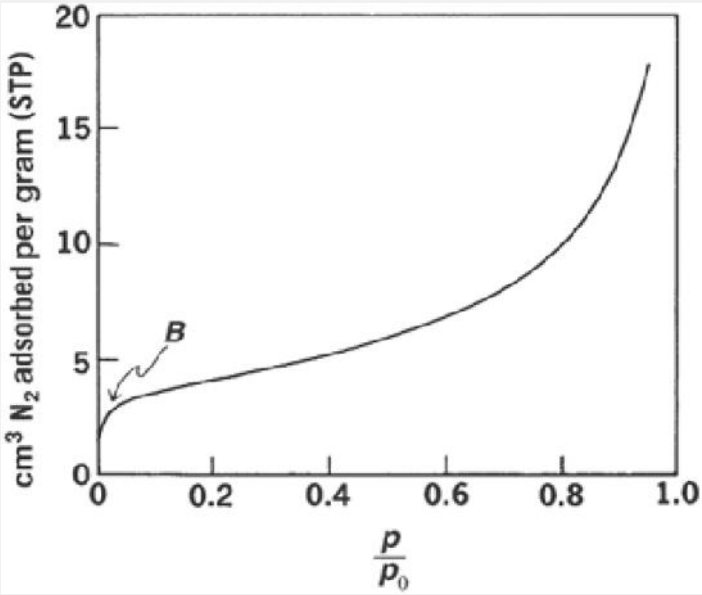

Fig. 18-10. Isotherm showing the volume of nitrogen adsorbed on a powder at increasing pressure ratio. Point *B* represents the volume of adsorbed gas corresponding to the completion of a monomolecular film. Key: STP = standard temperature and pressure.

$$\frac{p}{V(p_0 - p)} = \frac{1}{V_m b} + \frac{(b-1)p}{V_m b p_0} \qquad \textbf{(18–18)}$$

where V is the volume of gas in cm^3 adsorbed per gram of powder at pressure p, p_0 is the saturation vapor pressure of liquefied nitrogen at the temperature of the experiment, and b is a constant that expresses the difference between the heat of adsorption and heat of liquefaction of the adsorbate (nitrogen). Note that at $p/p_0 = 1$, the vapor pressure, p, is equal to the saturation vapor pressure.

An instrument used to obtain the data needed to calculate surface area and pore structure of pharmaceutical powders is the Quantasorb QS-16, manufactured by the Quantachrome Corporation (Boynton, FL). Absorption and desorption of nitrogen gas on the powder sample is measured with a thermal conductivity detector when a mixture of helium and nitrogen is passed through a cell containing the powder. Nitrogen is the absorbate gas; helium is inert and is not adsorbed on the powder surface. A Gaussian or bell-shaped curve is plotted on a strip-chart recorder, the signal height being proportional to the rate of absorption or desorption of nitrogen and the area under the curve being proportional to the gas adsorbed on the particles. Quantasorb and similar instruments have replaced the older vacuum systems constructed of networks of glass tubing. These required long periods of time to equilibrate and were subject to leakage at valves and breaks in the glass lines. The sensitivity of the new instrument is such that small powder samples can be analyzed. Quantasorb's versatility allows the use of a number of individual gases or mixtures of gases as adsorbates over a range of temperatures. The instrument can be used to measure the true density of powdered material and to obtain pore-size and pore-volume distributions. The characteristics of porous materials and the method of analysis are discussed in the following sections.

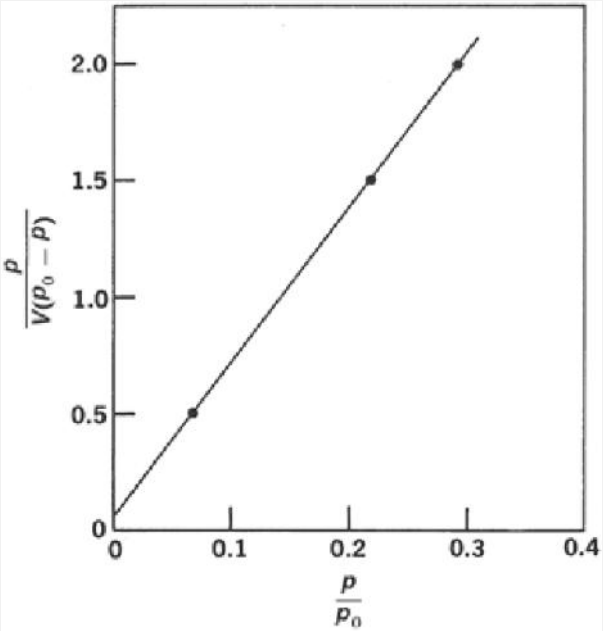

Fig. 18-11. A linear plot of the Brunaver, Emmett, and Teller (BET) equation for the adsorption of nitrogen on a powder.

Instead of the graph shown in Figure 18-10, a plot of $p/V(p_0 - p)$ against p/p_0, as shown in Figure 18-11, is ordinarily used to obtain a straight line, the slope and intercept of which yield the values b and V_m. The specific surface of the particles is then obtained from

$$S_w = \frac{A_m N}{M/\rho} \times V_m \text{ cm}^3/\text{g}$$

$$S_w = \frac{(16.2 \times 10^{-16})(6.02 \times 10^{23})}{22.414 \times 10^4} \times V_m$$

$$S_w = 4.35 \text{ m}^2/\text{cm}^3 \times V_m \text{ cm}^3/\text{g} \qquad \textbf{(18–19)}$$

where M/σ is the molar volume of the gas, 22,414 cm^3/mole at standard temperature and pressure (STP), and the factor 10^4 is included in the denominator to convert square centimeters to square meters. N is Avogadro's number, 6.02×10^{23} molecules/mole, and A_m is the area of a single close-packed nitrogen molecule adsorbed as a monolayer on the surface of the particles. Emmett and Brunauer29 suggested that the value of A_m for nitrogen be calculated from the formula

$$A_m = 1.091 \left(\frac{M}{\rho N}\right)^{2/3} \qquad \textbf{(18–20)}$$

where M is the molecular weight, 28.01 g/mole, of N_2; σ is the density, 0.81 g/cm^3, of N_2 at its boiling point, 77 K (-196°C); and N is Avogadro's number. The quantity 1.091 is a packing factor for the nitrogen molecules on the surface of the adsorbent. We have

$$A_m = 1.091 \left(\frac{28.01 \text{ g/mole}}{(0.81 \text{ g/cm}^3)(6.02 \times 10^{23} \text{ molecules/mole})}\right)^{2/3}$$

$$= 16.2 \times 10^{-16} \text{ cm}^2 = 16.2 \text{ Å}^2$$

A_m for liquid nitrogen has been obtained by several methods and is generally accepted as 16.2 $Å^2$, or 16.2×10^{-16} cm^2. The specific surface is calculated from equation (18-19) and is expressed in square meters per gram.

Experimentally, the volume of nitrogen that is adsorbed by the powder contained in the evacuated glass bulb of the Quantasorb or similar surface-area apparatus is determined at various pressures and the results are plotted as shown in Figure 18-11. The procedure was developed by Brunauer, Emmett, and Teller30 and is commonly known as the *BET method*. It is discussed in some detail by Hiemenz and by Allen.31 Swintosky et al.32 used the procedure to determine the surface area of pharmaceutical powders. They found the specific surface of zinc oxide to be about 3.5 m^2/g; the value for barium sulfate is about 2.4 m^2/g.

Example 18-7

Specific Surface

Using the Quantasorb apparatus, a plot of $p/V(p_0 - p)$ versus p/p_0 was obtained as shown in Figure 18-11 for a new antibiotic powder. Calculate S_w, the specific surface of the powder, in m^2/g. The data can be read from the graph to obtain the following values:

$p/V(p_0 - p)$	0.05	0.150	0.20
p/p_0	0.07	0.220	0.290

Following the BET equation (18-18) and using linear regression, the intercept, $1/(V_m b)$, is I = 0.00198 and the slope $(b - 1)/(V_m b)$ is S = 0.67942. By rearranging equation (18-18), we find V_m:

$$V_m = \frac{1}{1 + S} = \frac{1}{0.00198 + 0.67942}$$

$$= 1.46757 \text{ cm}^3/\text{g}$$

The specific surface, S_w, is obtained using equation (18-19):

$$S_w = 4.35 \text{ m}^2/\text{cm}^3 \times V_m \text{ cm}^3/\text{g} = 6.38 \text{ m}^2\text{g}^{-1}$$

Assuming that the particles are spherical, we can calculate the mean volume–surface diameter by use of equation (18-17):

$$d_{vs} = \frac{6}{\rho S_w}$$

where ρ is the density of the adsorbent and S_w is the specific surface in square centimeters per gram of adsorbent. Employing this method, Swintosky et al.32 found the mean volume–surface diameter of zinc oxide particles to be 0.3 μm.

Air Permeability Method

The principal resistance to the flow of a fluid such as air through a plug of compacted powder is the surface area of the powder. The greater is the surface area per gram of powder, S_w, the greater is the resistance to flow. Hence, for a given pressure drop across the plug, permeability is inversely proportional to specific surface; measurement of the former provides a means of estimating this parameter. From equation **(**18-16**)** or **(**18-17**)**, it is then possible to compute d_{vs}.

A plug of powder can be regarded as a series of capillaries whose diameter is related to the average particle size. The

internal surface of the capillaries is a function of the surface area of the particles. According to Poiseuille equation,

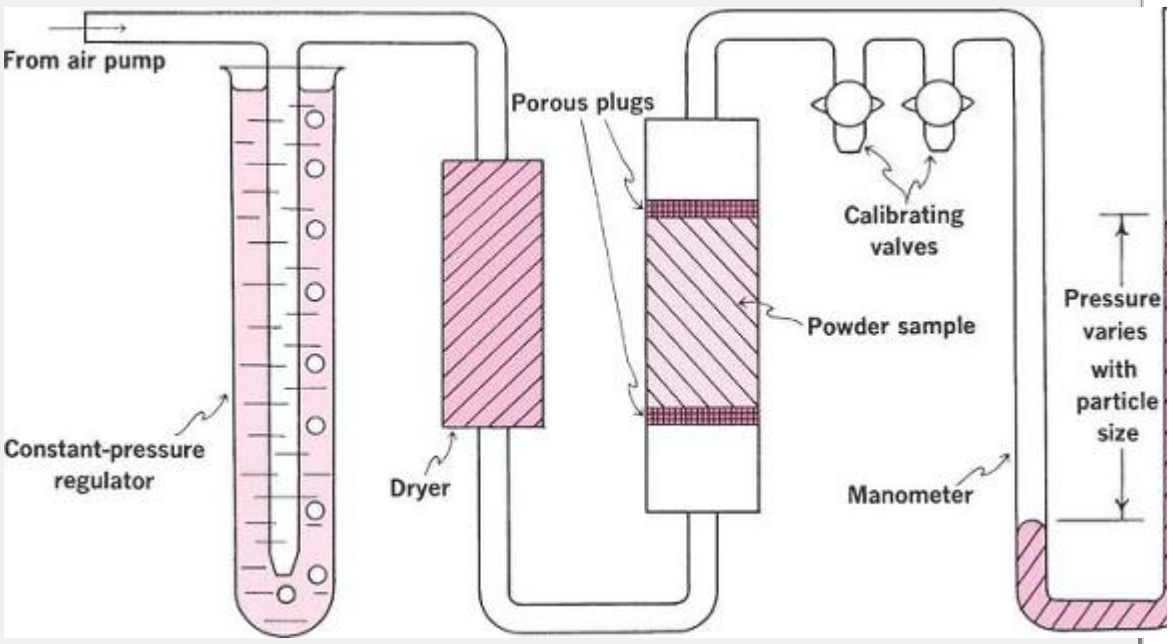

Fig. 18-12. The Fisher subsieve sizer. An air pump generates air pressure to a constant head by means of the pressure regulator. Under this head, the air is dried and conducted to the powder sample packed in the tube. The flow of air through the powder bed is measured by means of a calibrated manometer and is proportional to the surface area or the average particle diameter.

$$V = \frac{\pi d^4 \Delta P t}{128 l \eta} \qquad (18\text{–}21)$$

where V is the volume of air flowing through a capillary of internal diameter d and length l in t seconds under a pressure difference of ΔP. The viscosity of the fluid (air) is η poise.

In practice, the flow rate through the plug, or bed, is also affected by (*a*) the degree of compression of the particles and (*b*) the irregularity of the capillaries. The more compact the plug, the lower is the*porosity*, which is the ratio of the total space between the particles to the total volume of the plug. The irregularity of the capillaries means that they are longer than the length of the plug and are not circular.

The Kozeny–Carman equation, derived from the Poiseuille equation, is the basis of most air permeability methods. Stated in one form, it is

$$V = \frac{A}{\eta S_w^2} \cdot \frac{\Delta P t}{K l} \cdot \frac{\varepsilon^3}{(1-\varepsilon)^2} \qquad \textbf{(18–22)}$$

where A is the cross-sectional area of the plug, K is a constant (usually 5.0 ± 0.5) that takes account of the irregular capillaries, and ε is the porosity. The other terms are as defined previously.

A commercially available instrument is the Fisher subsieve sizer. The principle of its operation is illustrated in Figure 18-12. This instrument was modified by Edmundson33 to improve its accuracy and precision.

Equation (18-22) apparently takes account of the effect of porosity on S_w or d_{vs}. It is frequently observed, however, that d_{vs} decreases with decreasing porosity. This is especially true of pharmaceutical powders that have diameters of a few micrometers. It is customary, therefore, in these cases to quote the minimum value obtained over a range of porosities as the diameter of the sample. This noncompliance with equation (18-22) probably arises from initial bridging of the particles in the plug to produce a nonhomogeneous powder bed.5 It is only when the particles are compacted firmly that the bed becomes uniform and d_{vs} reaches a minimum value.

Because of the simple instrumentation and the speed with which determinations can be made, permeability methods are widely used pharmaceutically for specific-surface determinations, especially when the aim is to control batch-to-batch variations. When using this technique for more fundamental studies, it would seem prudent to calibrate the instrument.

Bephenium hydroxynaphthoate, official in the 1973 *British Pharmaceutical Codex*, is standardized by means of an air permeability method. The drug, used as an anthelmintic and administered as a suspension, must possess a surface area of not less than 7000 cm^2/g. As the specific surface of the material is reduced, the activity of the drug also falls.

Seth et al.34a studied the air permeability method of the *U. S. Pharmacopeia*, 20th edition, which used a Fisher subsieve sizer for determining the specific surface area of griseofulvin (also see *U. S. Pharmacopeia*34b). The authors suggested improvements in the method, principal among which was the use of a defined porosity, such as 0.50. This specified value is used in the ASTM Standard C-204–79 (1979) for measuring the fineness of Portland cement.

The volume surface diameter, d_{vs}, and therefore the specific surface, S_w, or surface area per unit weight in grams [equation (18-19)] of a powder can be obtained by use of this instrument (see Fig. 18-12). It is based on measuring the flow rate of air through the powder sample. If the sample weight is made exactly equal to the density of the powder

sample, a more elaborate equation35,36 for the average particle diameter, d_{vs}, is reduced to the simple expression

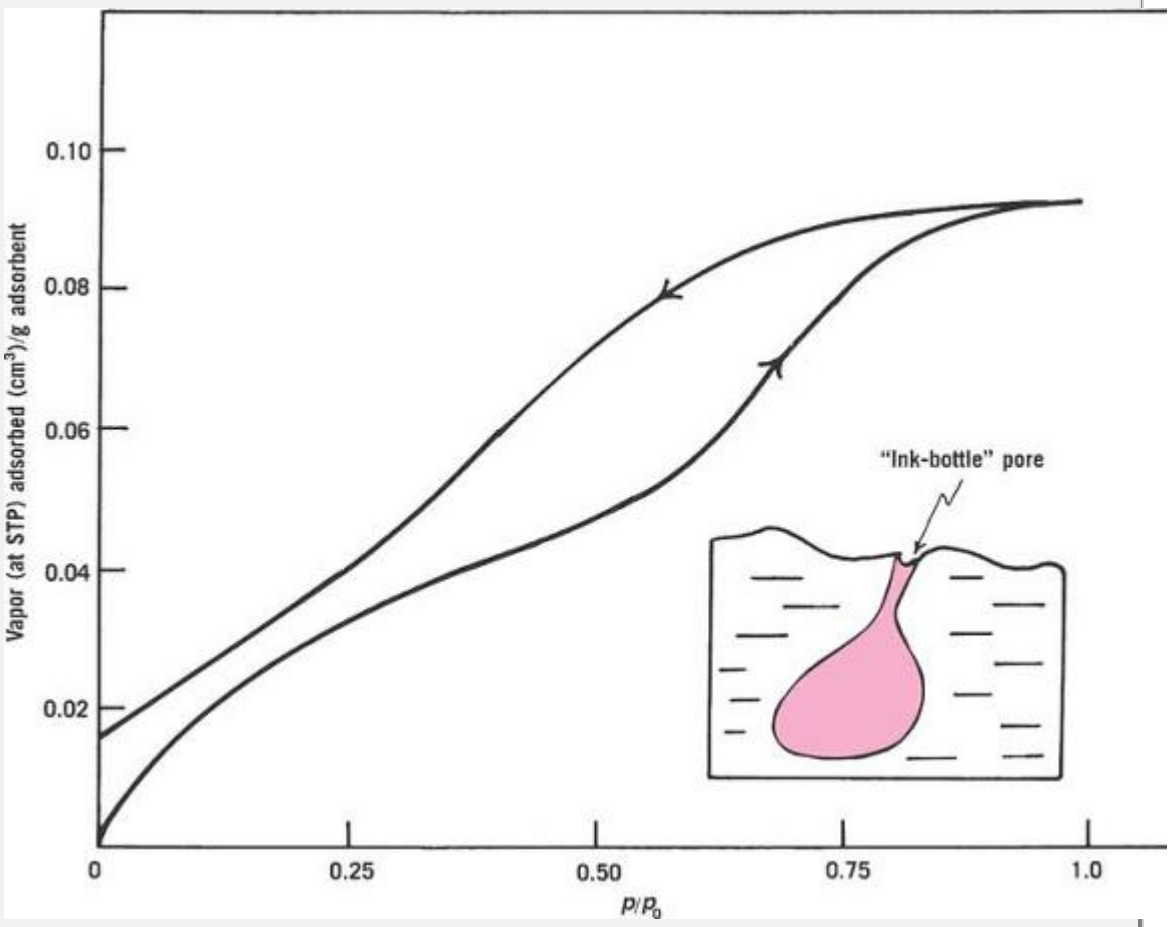

Fig. 18-13. Open hysteresis loop of an adsorption isotherm, presumably due to materials having "ink-bottle" pores, as shown in the inset. Key: STP = standard temperature and pressure.

$$d_{vs} = \frac{cL}{[(AL) - 1]^{3/2}} \cdot \sqrt{\frac{F}{P - F}} \qquad (18\text{–}23)$$

where *c* is an instrument constant, *L* is the sample height in cm, *A* is the cross-sectional area of the sample holder in cm^2, *F* is the pressure drop across a flowmeter resistance built into the instrument, and *P* is the air pressure as it enters the sample. The pressure (in cm of water) is measured with a water manometer rather than the better-known mercury manometer.

Pore Size

Materials of high specific area may have cracks and pores that adsorb gases and vapors, such as water, into their interstices. Relatively insoluble powdered drugs may dissolve more or less rapidly in aqueous medium depending on their adsorption of moisture or air. Other properties of pharmaceutical importance, such as the dissolution rate of drug from tablets, may also depend on the adsorption characteristics of drug powders. The adsorption isotherms for porous solids display hysteresis, as seen in Figures 18-13 and 18-14, in which the desorption or downcurve branch lies above and to the left of the adsorption or upcurve. In Figure 18-13, the open hysteresis loop is due to a narrow-neck or "ink-bottle" type of pore (see the inset in Fig. 18-13) that traps adsorbate, or to irreversible changes in the pore when adsorption of the gas has occurred so that desorption follows a different pattern than adsorption. The curve of Figure 18-14 with its closed hysteresis loop is more difficult to account for. Notice in Figures 18-13 and 18-14that at each relative pressure p/p_0, there are two volumes (at points*a* and *b* in Fig. 18-14) corresponding to a relative pressure *c*.

The upcurves of Figures 18-13 and 18-14 correspond to gas adsorption into the capillaries and the downcurve to desorption of the gas. A smaller volume of gas is adsorbed during adsorption (point *a* of Fig. 18-14) than is lost during desorption (point *b*). Vapor condenses to a liquid in small capillaries at a value less than p_0, the saturation vapor pressure, which can be taken as the vapor pressure at a flat surface. If the radius of the pore is *r* and the radius of the meniscus is *R* (Fig. 18-15, point *a*), p/p_0 can be calculated using expression known as the *Kelvin equation*,*

$$NkT \ln(p/p_0) = -\frac{2M\gamma}{\rho R} \qquad (18\text{–}24)$$

P.459

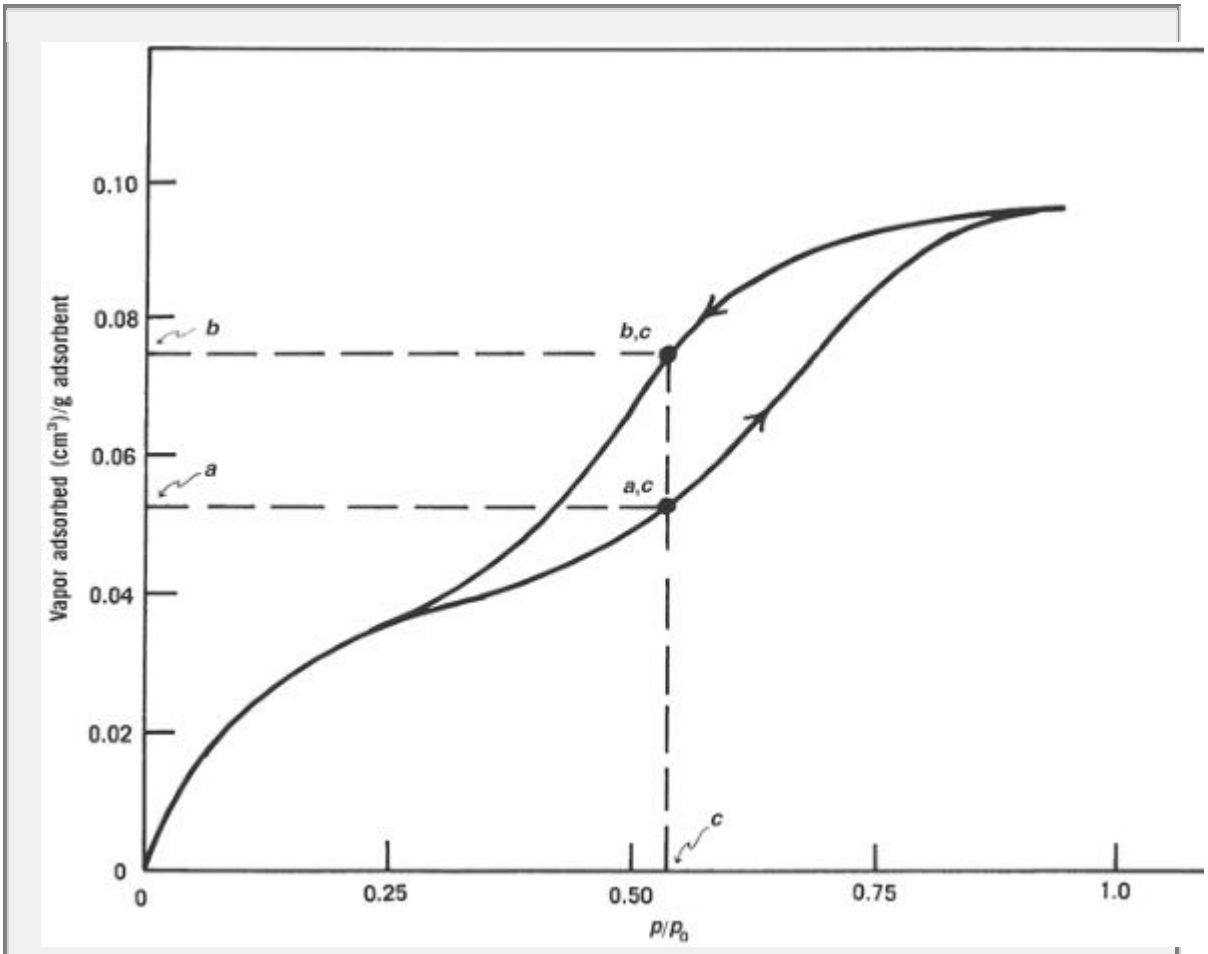

Fig. 18-14. Closed hysteresis loop of the adsorption isotherm of a porous material. At$p/p_0 = c$ on the curve of the loop, the volume of the pore is given by point *a*. At relative pressure *c* on the downcurve of the pore, volume is given by point *b*.

where *M* is molecular weight of the condensing gas and ρ is its density at a particular temperature, M/σ is the molar volume of the fluid and γ is its surface tension, *N* is Avogadro's number, and *k* is the Boltzmann constant, 1.381×10^{-16} erg/deg molecule. If the condensing vapor is water with a density of 0.998 at 20°C and a surface tension of 72.8 ergs/cm^2 and if the radius of the meniscus in the capillary *R* is 1.67×10^{-7} cm, we can calculate p/p_0 to be

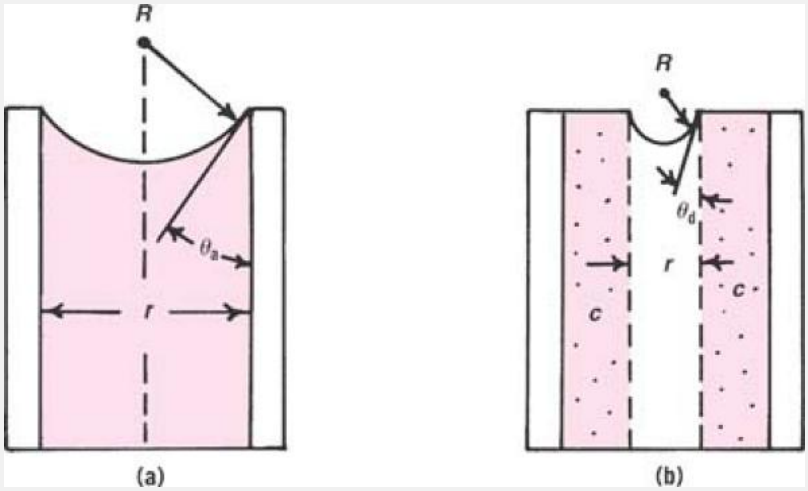

Fig. 18-15. (*a*) Pore into which vapor is condensing, corresponding to point *a, c* on the upcurve of Figure 18-14. Key: θ_a = advancing contact angle; *r* = pore radius; *R*= radius of meniscus. (*b*) Pore from which the liquid is vaporizing, corresponding to point *b, c* on the downcurve of Figure 18-14. Key: θ_d = receding or desorption contact angle; *R* and *R* are defined as in (*a*); *c* = condensed vapor on walls of the capillary.

$$\ln \frac{p}{p_0} = -\frac{2(18.015 \text{ g/mole})(72.8 \text{ ergs/cm}^2)}{(6.022 \times 10^{23} \text{ molecules/mole})} \times 1/[(1.381 \times 10^{-16} \text{ erg/deg molecules})] \times 1/[(0.998 \text{ g/cm}^3)(1.67 \times 10^{-7} \text{ cm})(293.18 \text{ K})]$$

$$\ln \frac{p}{p_0} = -0.6455$$

$$\frac{p}{p_0} = 0.5244$$

During adsorption, the capillary is filling (point *a, c* in Fig. 18-14) and the contact angle, θ_a (advancing contact angle), is greater than that during desorption, θ_d, at which time the capillary is emptying. The radius of the meniscus will be smaller in the receding stage than in the advancing stage because the capillary is partly filled with fluid from multilayer adsorption. This smaller receding contact angle means a smaller radius of the meniscus, as seen in Figure 18-15b, and p/p_0 will decrease because *R* is in the denominator of the Kelvin equation, the right-hand side of which is negative.

Table 18-8 Water Adsorption and Desorption on a Clay as a Function of Relative Pressure, p/p_0

	(1) p/p_0	(2) V_1(Absorption) (mL/g)	(3) V_2(Desorption) (mL/g)	(4) Radius (Å)	(5) Cumulative Pore Volume (%)
1	0.20	0.079	0.123	<6.7	54.9
2	0.31	0.109	0.147	<9.2	65.6
3	0.40	0.135	0.165	<11.7	73.7
4	0.49	0.141	0.182	<15.1	81.3
5	0.66	0.152	0.191	<30	85.3
6	0.80	0.170	0.200	<48.4	89.3
7	0.96	0.224	0.224	<265	100

The Kelvin equation gives a reasonable explanation for the differences of p/p_0 on adsorption and desorption and consequently provides for the existence of the hysteresis loop. The Kelvin equation, together with the hysteresis loops in adsorption–desorption isotherms (Fig. 18-14), can be used to compute the pore-size distribution.37 During desorption, at a given p/p_0 value, water will *condense* only in pores of radius equal to or below the value given by the Kelvin equation. Water will *evaporate* from pores of larger radius. Thus, from the desorption isotherm, the volume of water retained at a given pressure p/p_0 corresponds to the volume of pores having radius equal to or below the radius calculated from the Kelvin equation at this p/p_0 value.

Example 18-8
Pore Radius

Yamanaka et al.38 obtained experimental values for a water adsorption–desorption isotherm at 20°C on a clay. These values, which are given in Table 18-8, are selected from Figure 7 of their work.38

(*a*) Compute the radius of pores corresponding to the relative pressures p/p_0 given in Table 18-8.

(*b*) Assuming that all pores are of radius less than 265 Å, compute the cumulative percentage of pore volume with radii less than those found in part (*a*).

(*c*) Compute the percentage of pore volume at 20°C with radii between 40 and 60 Å.

(*a*) Using the Kelvin equation for $p/p_0 = 0.2$, we obtain

$$R = -2\gamma V([RT\ln(p/p_0)]$$

$$= -\frac{2 \times 72.8 \times 18}{(8.3143 \times 10^7 \times 293)(\ln 0.2)}$$

$$= (+)6.7 \times 10^{-8}\ \text{cm} = 6.7\ \text{Å}$$

The results for the several p/p_0 values are shown in the fourth column of Table 18-8.

(*b, c*) The total cumulative pore volume is 0.224 mL/g, corresponding to the intersection of the adsorption and desorption curves (row 7 in Table 18-8). It corresponds to 100% cumulative pore volume. Therefore, for, say, pores of radius less than 48.4 Å (Table 18-8, column 4, row 6), the cumulative percentage of pore volume is

$$\% = \frac{0.200}{0.224} \times 100 = 89.3\%$$

where the value 0.200 mL/g is taken from the desorption isotherm (Table 18-8, column 3, row 6). The results are given in column 5 of Table 18-8.

Christian and Tucker39 made a careful and extensive study of pore models and concluded that a model that included a combination of cylindrical and slit-shaped pores provided the best quantitative fit of the data obtained on both the adsorption and desorption branches of the pore distribution plots. A modification of the BET equation assuming multilayer adsorption at the capillary walls has also been found to provide a satisfactory model for the hysteresis that occurs with porous solids.40

The adsorption of water vapor, flavoring agents, perfumes, and other volatile substances into films, containers, and other polymeric materials used in pharmacy is important in product formulation and in the storage and use of drug products. Sadek and Olsen41showed that the adsorption isotherms for water vapor on methylcellulose, povidone, gelatin, and polymethylmethacrylate all exhibited hysteresis loops. Hydration of gelatin films was observed to be lowered by treatment with formaldehyde, which causes increased cross-linking in gelatin and a decrease in pore size. Povidone showed increased water adsorption on treatment with acetone, which enlarged pore size and increased the number of sites for water sorption. In a study of the action of tablet disintegrants, Lowenthal and Burress42 measured the mean pore diameter of tablets in air permeability apparatus. A linear correlation was observed between log mean pore diameter and tablet porosity, allowing a calculation of mean pore diameter from the more easily obtained tablet porosity. Gregg and Sing43 discussed pore size and pore-size distribution in some detail.

Derived Properties of Powders

The preceding sections of this chapter have been concerned mainly with size distribution and surface areas of powders. These are the two *fundamental* properties of any collection of particles. There are, in addition, numerous *derived* properties that are based on these fundamental properties. Those of particular relevance to pharmacy are discussed in the remainder of this chapter. Very important properties, those of particle dissolution and dissolution rate, are subjects of separate chapters.

Porosity

Suppose a powder, such as zinc oxide, is placed in a graduated cylinder and the total volume is noted. The volume occupied is known as the *bulk volume*, V_b. If the powder is nonporous, that is, has no internal pores or capillary spaces, the bulk volume of the powder consists of the true volume of the solid particles plus the volume of the spaces between the particles. The volume of the spaces, known as the *void volume*, *v*, is given by the equation

$$v = V_b - V_p \qquad (18\text{–}25)$$

where V_p is the *true volume* of the particles. The method for determining the volume of the particles will be given later.

The *porosity* or *voids* ε of the powder is defined as the ratio of the void volume to the bulk volume of the packing:

$$\varepsilon = \frac{V_b - V_p}{V_b} = 1 - \frac{V_p}{V_b} \qquad (18\text{–}26)$$

Porosity is frequently expressed in percent, $\varepsilon \times 100$.

Example 18-9
Calculate Porosity

A sample of calcium oxide powder with a true density of 3.203 and weighing 131.3 g was found to have a bulk volume of 82.0 cm^3 when placed in a 100 mL graduated cylinder. Calculate the porosity.

The volume of the particles is

$$131.3\ \text{g}/(3.203\ \text{g/cm}^3) = 41.0\ \text{cm}^3$$

From equation (18-25), the volume of void space is

$$v = 82.0\ \text{cm}^3 - 41.0\ \text{cm}^3 = 41.0\ \text{cm}^3$$

and from equation (18-26) the porosity is

$$\epsilon = \frac{82 - 41}{82} = 0.5 \text{ or } 50\%$$

Packing Arrangements

Powder beds of uniform-sized spheres can assume either of two ideal packing arrangements: (*a*) *closest* or *rhombohedral* and (*b*)*most open, loosest*, or *cubic packing*. The theoretical porosity of a powder consisting of uniform spheres in closest packing is 26% and for loosest packing is 48%. The arrangements of spherical particles in closest and loosest packing are shown in Figure 18-16.

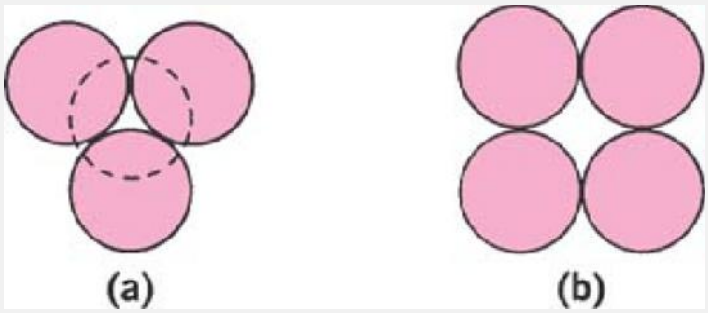

Fig. 18-16. Schematic representation of particles arranged in (*a*) closest packing and (*b*) loosest packet. The dashed circle in (*a*) shows the position taken by a particle in a plan above that of the other three particles.

The particles in real powders are neither spherical in shape nor uniform in size. It is to be expected that the particles of ordinary powders may have any arrangement intermediate between the two ideal packings of Figure 18-16, and most powders in practice have porosities between 30% and 50%. If the particles are of greatly different sizes, however, the smaller ones may shift between the larger ones to give porosities below the theoretical minimum of 26%. In powders containing flocculates or aggregates, which lead to the formation of bridges and arches in the packing, the porosity may be above the theoretical maximum of 48%. In real powder systems, then, almost any degree of porosity is possible. Crystalline materials compressed under a force of 100,000 lb/in.2 can have porosities of less than 1%.

Densities of Particles

Because particles may be hard and smooth in one case and rough and spongy in another, one must express densities with great care. Density is universally defined as weight per unit volume; the difficulty arises when one attempts to determine the volume of particles containing microscopic cracks, internal pores, and capillary spaces.

For convenience, three types of densities can be defined43'44: (*a*)*the true density* of the material itself, exclusive of the voids and intraparticle pores larger than molecular or atomic dimensions in the crystal

lattices, (*b*) the *granule density* as determined by the displacement of mercury, which does not penetrate at ordinary pressures into pores smaller than about 10 μm, and (*c*) the *bulk density* as determined from the bulk volume and the weight of a dry powder in a graduated cylinder.*

When a solid is nonporous, true and granule densities are identical, and both can be obtained by the displacement of helium or a liquid such as mercury, benzene, or water. When the material is porous, having an internal surface, the true density is best approximated by the displacement of helium, which penetrates into the smallest pores and is not adsorbed by the material. The density obtained by liquid displacement is considered as approximately equal to true density but may

differ from it somewhat when the liquid does not penetrate well into the pores.

The methods for determining the various densities are now discussed. *True density*, ρ, is the density of the actual solid material. Methods for determining the density of nonporous solids by displacement in liquids in which they are insoluble are found in general pharmacy books. If the material is porous, as is the case with most powders, the true density can be determined by use of a helium densitometer, as suggested by Franklin.45 The volume of the empty apparatus (dead space) is first determined by introducing a known quantity of helium. A weighed amount of powder is then introduced into the sample tube, adsorbed gases are removed from the powder by an outgassing procedure, and helium, which is not adsorbed by the material, is again introduced. The pressure is read on a mercury manometer, and by application of the gas laws, the volume of helium surrounding the particles and penetrating into the small cracks and pores is calculated. The difference between the volume of helium filling the empty apparatus and the volume of helium in the presence of the powder sample yields the volume occupied by the powder. Knowing the weight of the powder, one is then able to calculate the true density. The procedure is equivalent to the first step in the BET method for determining the specific surface area of particles.

The density of solids usually listed in handbooks is often determined by liquid displacement. It is the weight of the body divided by the weight of the liquid it displaces, in other words, the loss of weight of the body when suspended in a suitable liquid. For solids that are insoluble in the liquid and heavier than it, an ordinary pycnometer can be used for the measurement. For example, if the weight of a sample of glass beads is 5.0 g and the weight of water required to fill a pycnometer is 50.0 g, then the total weight would be 55.0 g. When the beads are immersed in the water and the weight is determined at 25°C, the value is 53.0 g, or a displacement of 2.0 cm^3 of water, and the density is 5.0 g/2.00 cm^3 = 2.5 g/cm^3. The true density determined in this manner may differ slightly depending on the ability of the liquid to enter the pores of the particles, the possible change in the density of the liquid at the interface, and other complex factors.

Because helium penetrates into the smallest pores and crevices (Fig. 18-17), it is generally conceded that the helium method gives the closest approximation to true density. Liquids such as water and alcohol are denied entrance into the smallest spaces, and liquid displacement accordingly gives a density somewhat smaller than the true value. True densities are given in Table 18-9 for some powders of pharmaceutical interest.

Granule density, ρ_g, can be determined by a method similar to the liquid displacement method. Mercury is used because it fills the void spaces but fails to penetrate into the internal pores of the particles. The volume of the particles together with their *intraparticle spaces*then gives the granule volume, and from a knowledge of the powder weight, one finds the granule density. Strickland et al.46 determined the granule density of tablet granulations by the mercury displacement method, using a specially designed pycnometer. A measure of true density was obtained by highly compressing the powders. The samples were compressed to 100,000 lb/in2, and the resulting tablets were weighed. The volumes of the tablets were computed after measuring the tablet dimensions with calipers. The weight of the tablet divided by the volume then gave the “true” or high-compression density.

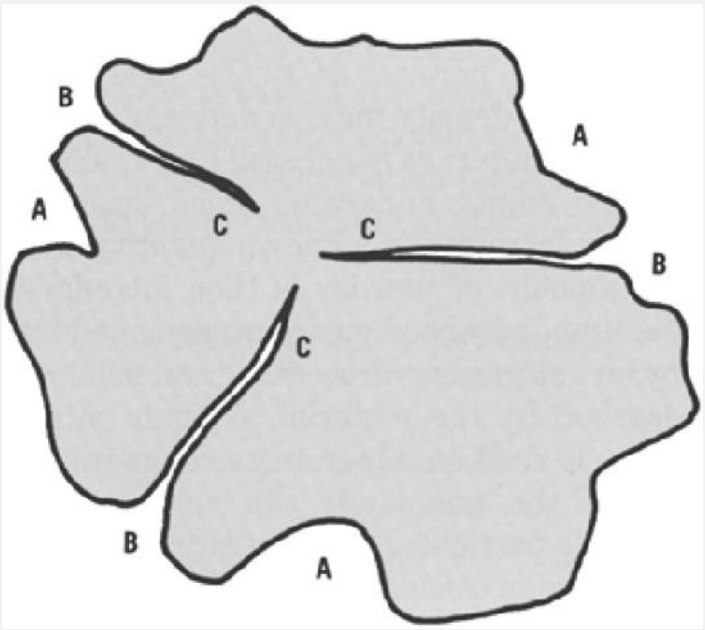

Fig. 18-17. Pores and crevices of a pharmaceutical granule. Water or mercury surrounds such a particle and rests only in the surface irregularities such as regions A and B. Helium molecules may enter deep into the cracks at points C, allowing calculation of true rather than granule density.

The *intraparticle porosity* of the granules can be computed from a knowledge of the true and granule density. The porosity is given by the equation

$$\varepsilon_{\text{intraparticle}} = \frac{V_g - V_p}{V_g} = 1 - \frac{V_p}{V_g}$$

$$= 1 - \frac{\text{Weight/True density}}{\text{Weight/Granule density}} \qquad \textbf{(18–27)}$$

or

$$\varepsilon_{\text{intraparticle}} = 1 - \frac{\text{Granule density}}{\text{True density}} = 1 - \frac{\rho_g}{\rho} \qquad \textbf{(18–28)}$$

where V_p is the true volume of the solid particles and V_g is the volume of the particles together with the intraparticle pores.

Example 18-10
Intraparticle Porosity

The granule density, ρ_g, of sodium bicarbonate is 1.450 and the true density, ρ, is 2.033. Compute the intraparticle porosity.

We have

$$\varepsilon_{\text{intraparticle}} = 1 - \frac{1.450}{2.033} = 0.286 \text{ or } 28.6\%$$

The granule densities and internal porosity or percent pore spaces in the granules, as obtained by Strickland et al.,46 are shown inTable 18-10. The difference in porosity depends on the method of granulation, as brought out in the table.

Table 18-9 True Density in g/cm^3 of Solids Commonly Used in Pharmacy

Aluminum oxide	4.0	Mercuric chloride	5.44
Benzoic acid	1.3	Mercuric iodide	6.3
Bismuth subcarbonate	6.86	Mercuric oxide	11.1
Bismuth subnitrate	4.9	Mercurous chloride	7.15
Bromoform	2.9	Paraffin	0.90
Calcium carbonate (calcite)	2.72	Potassium bromide	2.75
Calcium oxide	3.3	Potassium carbonate	2.29
Chalk	1.8–2.6	Potassium chloride	1.98
Charcoal (air free)	2.1–2.3	Potassium iodide	3.13
Clay	1.8–2.6	Sand, fine dry	1.5
Cork	0.24	Silver iodide	5.67
Cotton	1.47	Silver nitrate	4.35
Gamboge	1.19	Sodium borate, borax	1.73
Gelatin	1.27	Sodium bromide	3.2
Glass beads	2.5	Sodium chloride	2.16
Graphite	2.3–	Sucrose	1.6

	2.7		
Kaolin	2.2–2.5	Sulfadiazine	1.50
Magnesium carbonate	3.04	Sulfur, precipitated	2.0
Magnesium oxide	3.65	Talc	2.6–2.8
Magnesium sulfate	1.68	Zinc oxide (hexagonal)	5.59

Bulk density, ρ_b, is defined as the mass of a powder divided by the bulk volume. A standard procedure for obtaining bulk density or its reciprocal, *bulk specific volume*, has been established.47 A sample of about 50 cm^3 of powder that has previously been passed through a U. S. Standard No. 20 sieve is carefully introduced into a 100 mL graduated cylinder. The cylinder is dropped at 2 sec intervals onto a hard wood surface three times from a height of 1 in. The bulk density is then obtained by dividing the weight of the sample in grams by the final volume in cm^3 of the sample contained in the cylinder. The bulk density does not actually reach a maximum until the container has been dropped or tapped some 500 times; however, the three-tap method has been found to give the most consistent results among various laboratories. The bulk density of some pharmaceutical powders is compared with true and apparent densities in Table 18-11. The term “light” as applied to pharmaceutical powders means low bulk density or large bulk volume, whereas “heavy” signifies a powder of high bulk density or small volume. It should be noted that these terms have no relationship to granular or true densities.

Table 18-10 Densities and Porosities of Tablet Granulations*

Granulation	“True” or High-Compression Density (g/cm^3)	Granule Density by Mercury Displacement (g/cm^3)	Pore Space (Porosity)
Sulfathiazole†	1.530	1.090	29
Sodium bicarbonate†	2.033	1.450	29
Phenobarbital†	1.297	0.920	29
Aspirin‡	1.370	1.330	2.9

*From W. A. Strickland, Jr., L. W. Busse, and T. Higuchi, J. Am. Pharm. Assoc. Sci. Ed. **45,** 482, 1956. With permission.
†Granulation prepared by wet method using starch paste.
‡Granulation prepared by dry method (slugging process).

The bulk density of a powder depends primarily on particle-size distribution, particle shape, and the tendency of the particles to adhere to one another. The particles may pack in such a way as to leave large gaps between their surfaces, resulting in a light powder or powder of low bulk density. On the other hand, the smaller particles may shift between the larger ones to form a heavy powder or one of high bulk density.

The *interspace* or *void porosity* of a powder of porous granules is the relative volume of interspace voids to the bulk volume of the powder, exclusive of the intraparticle pores. The interspace porosity is computed from a knowledge of

the bulk density and the granule density and is expressed by the equation

Table 18-11 Comparison of Bulk Densities with True Densities

	Bulk Density (g/cm^3)	True Density (g/cm^3)
Bismuth subcarbonate heavy	1.01	6.9*
Bismuth subcarbonate light	0.22	6.9*
Magnesium carbonate heavy	0.39	3.0*
Magnesium carbonate light	0.07	3.0*
Phenobarbital	0.34	1.3†
Sulfathiazole	0.33	1.5†
Talc	0.48	2.7*

*Density obtained by liquid displacement.
†True density obtained by helium displacement.

$$\varepsilon_{\text{interspace}} = \frac{V_b - V_g}{V_b} = 1 - \frac{V_g}{V_b} = 1 - \frac{\text{Weight/Granule density}}{\text{Weight/Bulk density}} \qquad \textbf{(18–29)}$$

$$\varepsilon_{\text{interspace}} = 1 - \frac{\text{Bulk density}}{\text{Granule density}} = 1 - \frac{\rho_b}{\rho_g} \qquad \textbf{(18–30)}$$

where $V_b = w/\rho_b$ is the bulk volume and $V_g = w/\rho_g$ is the granule volume, that is, the volume of the particles plus pores.

The *total porosity* of a porous powder is made up of voids between the particles as well as pores within the particles. The total porosity is defined as

$$\varepsilon_{\text{total}} = \frac{V_b - V_p}{V_b} = 1 - \frac{V_p}{V_b} \qquad \textbf{(18–31)}$$

where V_b is the bulk volume and V_p is the volume of the solid material. This equation is identical with that for nonporous powders [equation (18-26)]. As in the previous cases, V_p and V_b can be expressed in terms of powder weights and densities:

$$V_p = \frac{w}{\rho}$$

and

$$V_b = \frac{w}{\rho_b}$$

where w is the mass ("weight") of the powder, ρ is the true density, and ρ_b is the bulk density. Substituting these relationships into equation (18-31) gives for the total porosity

$$\varepsilon_{\text{total}} = 1 - \frac{w/\rho}{w/\rho_b} \qquad \textbf{(18–32)}$$

or

$$\varepsilon_{\text{total}} = 1 - \frac{\rho_b}{\rho} \qquad \textbf{(18–33)}$$

Example 18-11
Bulk Density and Total Porosity

The weight of a sodium iodide tablet was 0.3439 g and the bulk volume was measured by use of calipers and found to be 0.0963 cm^3. The true density of sodium iodide is 3.667 g/cm^3. What is the bulk density and the total porosity of the tablet?

We have

$$\rho_b = \frac{0.3439}{0.0963} = 3.571 \text{ g/cm}^3$$

$$\varepsilon_{total} = 1 - \frac{3.571}{3.667}$$

$$= 0.026 \text{ or } 2.6\%$$

In addition to supplying valuable information about tablet porosity and its evident relationship to tablet hardness and disintegration time, bulk density can be used to check the uniformity of bulk chemicals and to determine the proper size of containers, mixing apparatus, and capsules for a given mass of the powder. These topics are considered in subsequent sections of this chapter.

In summary, the differences among the three densities (true, granule, and bulk) can be understood better by reference to their reciprocals: specific true volume, specific granule volume, and specific bulk volume.

The specific true volume of a powder is the volume of the solid material itself per unit mass of powder. When the liquid used to measure it does not penetrate completely into the pores, the specific volume is made up of the volume per unit weight of the solid material itself and the small part of the pore volume within the granules that is not penetrated by the liquid. When the proper liquid is chosen, however, the discrepancy should not be serious. Specific granule volume is the volume of the solid and essentially all of the pore volume within the particles. Finally, specific bulk volume constitutes the volume per unit weight of the solid, the volume of the*intra*particle pores, and the void volume or volume of *inter*particle spaces.

Example 18-12

Total Porosity

The following data apply to a 1 g sample of a granular powder:

$$\text{Volume of the solid alone} = 0.3 \text{ cm}^3/\text{g}$$

$$\text{Volume of intraparticle pores} = 0.1 \text{ cm}^3/\text{g}$$

$$\text{Volume of spaces between particles} = 1.6 \text{ cm}^3/\text{g}$$

(*a*) What are the specific true volume, V, the specific granule volume, V_g, and the specific bulk volume, V_b?

$$V = 0.3 \text{ cm}^3$$

$$V_g = V + \text{intraparticle pores}$$

$$= 0.3 + 0.1 = 0.4 \text{ cm}^3/\text{g}$$

$$V_b = V + \text{intraparticle pores} + \text{spaces between particles}$$

$$= 0.3 + 0.1 + 1.6$$

$$= 2.0 \text{ cm}^3/\text{g}$$

(*b*) Compute the total porosity, ε_{total}, the interspace porosity, $\varepsilon_{interspace}$, or void spaces between the particles, and the intraparticle porosity, $\varepsilon_{intraparticle}$, or pore spaces within the particles.

We have

$$\varepsilon_{total} = \frac{V_b - V_p}{V_b} = \frac{2.0 - 0.3}{2.0}$$

$$= 0.85 \text{ or } 85\%$$

$$\varepsilon_{interspace} = \frac{V_b - V_g}{V_b} = \frac{2.0 - 0.4}{2.0}$$

$$= 0.80 \text{ or } 80\%$$

$$\varepsilon_{intraparticle} = \frac{V_g - V_p}{V_g} = \frac{0.4 - 0.3}{0.4}$$

$$= 0.25 \text{ or } 25\%$$

Thus, the solid constitutes 15% of the total bulk and 85% is made up of void space; 80% of the bulk is contributed by the voids between the particles and 5% of the total bulk by the pores and crevices within the particles. These pores, however, contribute 25% to the volume of granules, that is, particles plus pores.

P.465

Bulkiness

Specific bulk volume, the reciprocal of bulk density, is often called*bulkiness* or *bulk*. It is an important consideration in the packaging of powders. The bulk density of calcium carbonate can vary from 0.1 to 1.3, and the lightest or bulkiest type would require a container about 13 times larger than that needed for the heaviest variety. Bulkiness increases with a decrease in particle size. In a mixture of materials of different sizes, however, the smaller particles shift between the larger ones and tend to reduce the bulkiness.

Flow Properties

A bulk powder is somewhat analogous to a non-Newtonian liquid, which exhibits plastic flow and sometimes dilatancy, the particles being influenced by attractive forces to varying degrees. Accordingly, powders may be *free-flowing* or *cohesive* (“sticky”). Neumann48discussed the factors that affect the flow properties of powders. Of special significance are particle size, shape, porosity and density, and surface texture. Those properties of solids that determine the magnitude of particle–particle interactions were reviewed by Hiestand.49

With relatively small particles (less than 10 μm), particle flow through an orifice is restricted because the cohesive forces between particles are of the same magnitude as gravitational forces. Because these latter forces are a function of the diameter raised to the third power, they become more significant as the particle size increases and flow is facilitated. A maximum flow rate is reached, after which the flow decreases as the size of the particles approaches that of the orifice.50 If a powder contains a reasonable number of small particles, the powder's flow properties may be improved be removing the “fines” or adsorbing them onto the larger particles. Occasionally, poor flow may result from the presence of moisture, in which case drying the particles will reduce the cohesiveness. A review by Pilpel51 deals with the various apparatus for the measurement of the properties of cohesive powders and the effects on cohesive powders of particle size, moisture, glidants, caking, and temperature.

Dahlinder et al.52 reviewed the methods for evaluating flow properties of powders and granules, including the *Hausner ratio* or packed bulk density versus loose bulk density, the rate of tamping, the flow rate and free flow through an orifice, and a “drained” angle of repose. The Hausner ratio, the free flow, and the angle of repose correlated well with one another and were applicable even for fairly cohesive tablet granulations.

Elongated or flat particles tend to pack, albeit loosely, to give powders with a high porosity. Particles with a high density and a low internal porosity tend to possess free-flowing properties. This can be offset by surface roughness, which leads to poor flow characteristics due to friction and cohesiveness.

Free-flowing powders are characterized by “dustibility,” a term meant to signify the opposite of stickiness. Lycopodium shows the greatest degree of dustibility; if it is arbitrarily assigned a dustibility of 100%, talcum powder has value of 57%, potato starch 27%, and fine charcoal 23%. Finely powdered calomel has a relative dustibility of 0.7%.48 These values should have some relation to the uniform spreading of dusting powders when applied to the skin, and stickiness, a measure of the cohesiveness of the particles of a compacted powder, should be of some importance in the flow of powders through filling machines and in the operation of automatic capsule machines.

Poorly flowing powders or granulations present many difficulties to the pharmaceutical industry. The production of uniform tablet dosage units has been shown to depend on several granular properties. Arambulo and coworkers53 observed that as the granule size was reduced, the variation in tablet weight fell. The minimum weight variation was attained with granules having a diameter of 400 to 800 μm. As

the granule size was reduced further, the granules flowed less freely and the tablet weight variation increased. The particle-size distribution affects the internal flow and segregation of a granulation. Raff et al.54 studied the flow of tablet granulations. They found that internal flow and granule demixing (i.e., the tendency of the powder to separate into layers of different sizes) during flow through the hopper contribute to a decrease in tablet weight during the latter portion of the compression period. Hammerness and Thompson55observed that the flow rate of a tablet granulation increased with an increase in the quantity of fines added. An increase in the amount of lubricant also raised the flow rate, and the combination of lubricant and fines appeared to have a synergistic action.

The frictional forces in a loose powder can be measured by the*angle of repose*, φ. This is the maximum angle possible between the surface of a pile of powder and the horizontal plane. If more material is added to the pile, it slides down the sides until the mutual friction of the particles, producing

a surface at an angle φ, is in equilibrium with the gravitational force. The tangent of the angle of repose is equal to the coefficient of friction, μ, between the particles:

$$\tan\phi = \mu \qquad (18\text{–}34)$$

Hence, the rougher and more irregular the surface of the particles, the higher will be the angle of repose. This situation was observed by Fonner et al.,56 who, in studying granules prepared by five different methods, found the repose angle to be primarily a function of surface roughness. Ridgeway and Rupp57 studied the effect of particle shape on powder properties. Using closely sized batches of sand separated into different shapes, they showed that, with increasing departure from the spherical, the angle of repose increased while bulk density and flowability decreased.

To improve flow characteristics, materials termed *glidants* are frequently added to granular powders. Examples of commonly used glidants are magnesium stearate, starch, and talc. Using a recording powder flowmeter that measured the weight of powder flowing per unit time through a hopper orifice, Gold et al.58 found the optimum glidant concentration to be 1% or less. Above this level, a decrease in flow rate was usually observed. No correlation was found between flow rate and repose angle. By means of a shear cell and a tensile tester, York59 was able to determine an optimum glidant concentration for lactose and calcium hydrogen phosphate powders. In agreement with the result of Gold et al.,58 the angle of repose was found to be unsuitable for assessing the flowability of the powders used.

Nelson60 studied the repose angle of a sulfathiazole granulation as a function of average particle size, presence of lubricants, and admixture of fines. He found that, in general, the angle increased with decreasing particle size. The addition of talc in low concentration decreased the repose angle, but in high concentration it increased the angle. The addition of fines—particles smaller than 100 mesh—to coarse granules resulted in a marked increase of the repose angle.

The ability of a powder to flow is one of the factors involving in mixing different materials to form a powder blend. Mixing, and the prevention of unmixing, is an important pharmaceutical operation involved in the preparation of many dosage forms, including tablets and capsules.61 Other factors affecting the mixing process are particle aggregation, size, shape, density differences, and the presence of static charge. Train62 and Fischer63 described the theory of mixing.

Compaction: Compressed Tablets

Neumann64 found that when powders were compacted under a pressure of about 5 kg/cm^2, the porosities of the powders composed of rigid particles (e.g., sodium carbonate) were higher than the porosities of powders in closest packing, as determined by tapping experiments. Hence, these powders were *dilatant*, that is, they showed an unexpected expansion, rather than contraction, under the influence of stress. In the case of soft and spongy particles (e.g., kaolin), however, the particles deformed on compression, and the porosities were lower than after tapping the powder down to its condition of closest packing. Similar experiments might be conducted to determine the optimum condition for packing powders into capsules on the manufacturing scale.

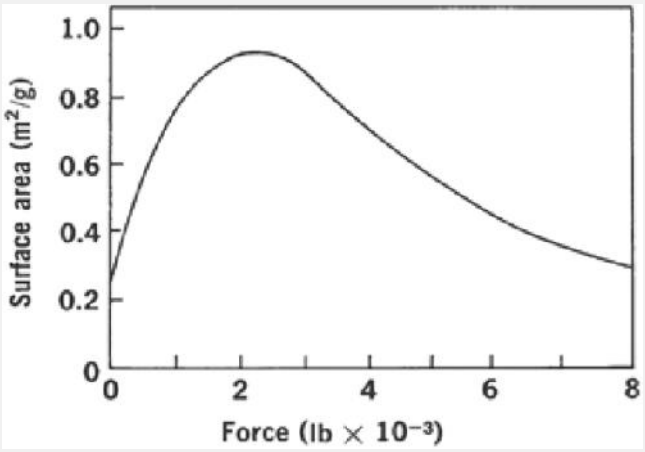

Fig. 18-18. The influence of compressional force on the specific surface of a sulfathiazole granulation. (From T. Higuchi et al., J. Am. Pharm. Assoc. Sci. Ed. **41,** 93, 1952; J. Am. Pharm. Assoc. Sci. Ed. **42,** 1944, 1953; J. Am. Pharm. Assoc. Sci. Ed. **43,** 344, 596, 685, 718, 1954; J. Am. Pharm. Assoc. Sci. Ed. **44,** 223, 1955; J. Am. Pharm. Assoc. Sci. Ed. **49,** 35, 1960; J. Pharm. Sci. **52,** 767, 1963.)

The behavior of powders under compression is significant in pharmaceutical tableting. Although basic information can be obtained from the literature on powder metallurgy and the compression of metallic powders, Train,65 who performed some of the fundamental work in this area, pointed out that not all the theories developed for the behavior of metals will necessarily hold when applied to nonmetals.

Much of the early work was carried out by Higuchi and associates,66who studied the influence of compression force on the specific surface area, granule density, porosity, tablet hardness, and disintegration time of pharmaceutical tablets. As illustrated in Figure 18-18, the specific surface of a sulfathiazole tablet granulation as determined by the BET method increased to a maximum and then decreased. The initial increase in surface area can be attributed to the formation of new surfaces as the primary crystalline material is fragmented, whereas the decrease in specific surface beyond a compression force of 2500 lb is presumably due to cold bonding between the unit particles. It was also observed that porosity decreased and density increased as a linear function of the logarithm of the compression force, except at the higher force levels. As the compression increased, the tablet hardness and fracture resistance also rose. Typical results obtained using an instrumented rotary tablet machine67 are shown in Figure 18-19.

The strength of a compressed tablet depends on a number of factors, the most important of which are compression force and particle size. The literature dealing with the effect of particle size has been outlined by Hersey et al.,68 who, as a result of their studies, concluded that, over the range 4 to 925 μm, there is no simple relationship between strength and particle size. These workers did find that for simple crystals,

the strength of the tablet increased with decreasing particle size in the range of 600 to 100 μm.

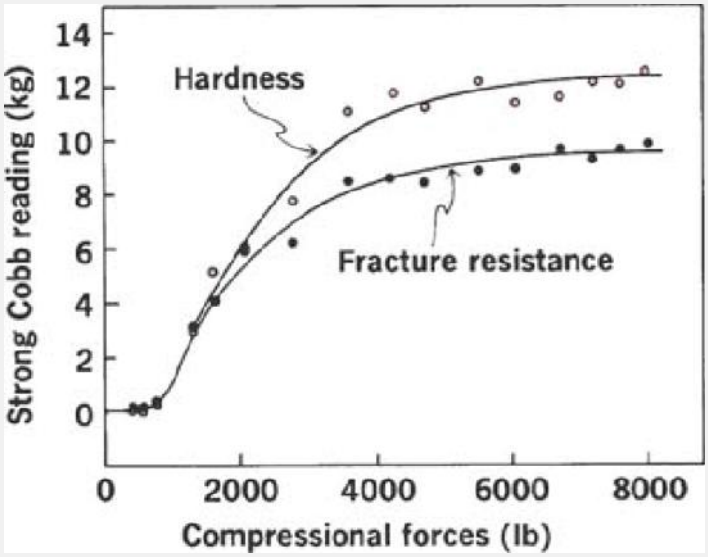

Fig. 18-19. Effect of compressional force on tablet hardness and fracture strength. (From E. L. Knoechel, C. C. Sperry, and C. J. Lintner, J. Pharm. Sci. **56,** 116, 1967.)

The work initiated by Higuchi and coworkers66 involved the investigation of other tablet ingredients, the development of an instrumented tablet machine, and the evaluation of tablet lubricants. The reader who desires to follow this interesting work should consult the original reports, as well as other studies69,70,71,72,73in this area. Tableting research and technology were comprehensively reviewed in 1972 by Cooper and Rees.74Deformation processes during decompression may be the principal factors responsible for the success or failure of compact formation.75

Chapter Summary

Knowledge and control of the size and the size range of particles are of profound importance in pharmacy. At this point you should understand that particle size is related in a significant way to the physical, chemical, and pharmacologic properties of a drug. Clinically, the particle size of a drug can affect its release from dosage forms that are administered orally, parenterally, rectally, and topically. The successful formulation of suspensions, emulsions, and tablets, from the viewpoints of both physical stability and pharmacologic response, also depends on the particle size achieved in the product. The student should have an understanding of the common particle sizes of pharmaceutical preparations and their impact on pharmaceutical processing/preparation; be familiar with the units for particle size, area, and volume and typical calculations; and be able to describe how particles can be characterized and why these methods are important. In the area of tablet and capsule manufacture, control of the particle size is essential in achieving the necessary flow properties and proper mixing of granules and powders.

Practice problems for this chapter can be found at thePoint.lww.com/Sinko6e.

References

1. K. A. Lees, J. Pharm. Pharmacol. **15,** 43T, 1963.
2. J. M. Dalla Valle, *Micromeritics*, 2nd Ed., Pitman, New York, 1948, p. xiv.
3. Seradyn, Particle Technology Division, 1200 Madison Ave., Box 1210, Indianapolis, In., 46206.
4. Duke Scientific, 1135D San Antonio Road, Palo Alto, Calif., 94303.
5. I. C. Edmundson, in H. S. Bean, J. E. Carless, and A. H. Beckett (Eds.), *Advances in Pharmaceutical Sciences*, **Vol. 2**, Academic Press, New York, 1967, p. 95.
6. E. L. Parrott, J. Pharm. Sci. **63,** 813, 1974.

7. A. Sano, T. Kuriki, T. Handa, H. Takeuchi, and Y. Kawashima, J. Pharm. Sci. **76,** 471, 1987.
8. T. Hatch, J. Franklin. Inst. **215,** 27, 1933; T. Hatch and S. P. Choate, J. Franklin. Inst. **210,** 793, 1930.
9. H. L. Rao, *Private Communication*, Manipal, India, 1986,
10. T. Allen, *Particle Size Measurement*, 2nd Ed., Chapman Hall, London, 1974.
11. M. J. Groves, Pharm. Tech. **4,** 781, 1980.
12. G. Martin, Br. Ceram. Soc. Trans. **23,** 61, 1926; Br. Ceram. Soc. Trans. **25,** 51, 1928; Br. Ceram. Soc. Trans. **27,** 285, 1930.
13. T. Allen, *Particle Size Measurement*, 2nd Ed., Chapman Hall, London, 1974, p. 131.
14. K. P. P. Prasad and L. S. C. Wan, Pharm. Res. **4,** 504, 1987.
15. A. S. Arambulo and D. L. Deardorff, J. Am. Pharm. Assoc. Sci. Ed. **42,** 690, 1953.
16. L. D. King and C. H. Becker, Drug Standards **21,** 1, 1953.
17. G. Herdan, *Small Particle Statistics,* Elsevier, New York, 1953, p. 72.
18. D. E. Fonner, Jr., G. S. Banker, and J. Swarbrick, J. Pharm. Sci. **55,** 576, 1966.
19. H. J. Heywood, J. Pharm. Pharmacol. **15,** 56T, 1963.
20. W. I. Higuchi et al., J. Pharm. Sci. **51,** 1081, 1962; J. Pharm. Sci. **52,** 162, 1963; J. Pharm. Sci. **53,** 405, 1964; J. Pharm. Sci.**54,** 74, 1205, 1303, 1965.
21. S. Bisaillon and R. Tawashi, J. Pharm. Sci. **65,** 222, 1976.
22. E. R. Garrett, G. H. Miller, and M. R. W. Brown, J. Pharm. Sci.**55,** 593, 1966; G. H. Miller, S. Khalil, and A. Martin, J. Pharm. Sci. **60,** 33, 1971.
23. L. J. Beaubien and A. J. Vanderwielen, J. Pharm. Sci. **69,**651, 1980.
24. S. I. Ismail and R. Tawashi, J. Pharm. Sci. **69,** 829, 1980.
25. E. C. Signoretti, A. Dell'Utri, L. Paoletti, D. Bastisti, and L. Montanari, Drug Dev. Ind. Pharm. **14,** 1, 1988.
26. S. P. Li, K. M. Feld, and C. R. Kowarski, Drug Dev. Ind. Pharm. **15,** 1137, 1989.
27. M. C. Davies, I. B. Wilding, R. D. Short, M. A. Khan, J. F. Watts, and C. D. Melia, Int. J. Pharm. **57,** 183, 1989.
28. F. Carli and A. Motta, J. Pharm. Sci. **73,** 197, 1984.
29. P. H. Emmett and S. Brunauer, J. Am. Chem. Soc. **59,** 1553, 1937; S. J. Gregg and K. S. W. Sing, *Adsorption, Surface Area and Porosity*, 2nd Ed., Academic Press, New York, 1982, p. 62.
30. S. Brunauer, P. H. Emmett, and F. Teller, J. Am. Chem. Soc.**60,** 309, 1938.
31. P. C. Hiemenz, *Principles of Colloid and Surface Chemistry*, 2nd Ed., Marcel Dekker, New York, 1986, pp. 513–529; T. Allen, *Particle Size Measurement,* Chapman Hall, London, 1975, pp. 358–366.
32. J. V. Swintosky, S. Riegelman, T. Higuchi, and L. W. Busse, J. Am. Pharm. Assoc. Sci. Ed. **38,** 210, 308, 378, 1949.
33. I. C. Edmundson, Analyst (Lond.), **91,** 1082, 1966.
34. a: P. Seth, N. Moller, J. C. Tritsch, and A. Stamm, J. Pharm. Sci. **72,** 971, 1983; and b: *United States Pharmacopeia*, 22nd Ed., US Pharmacopeial Convention, Rockville, MD, 1990, pp. 616.
35. P. C. Carman, J. Soc. Chem. Ind. **57,** 225, 1938; F. M. Lea and R. W. Nurse, J. Soc. Chem. Ind. **58,** 277, 1939.
36. E. L. Gooden and C. M. Smith, Ind. Eng. Chem. Anal. Ed.**12,** 479, 1940.
37. J. T. Carstensen, *Solid Pharmaceutics: Mechanical Properties and Rate Phenomena,* Academic Press, New York, 1980, pp. 130–131.
38. S. Yamanaka, P. B. Malla, and S. Komarheni, J. Colloid Interface Sci. **134,** 51, 1990.

39. S. D. Christian and E. E. Tucker, Am. Lab. **13,** 42, 1981; Am. Lab. **13,** 47, 1981.
40. P. C. Hiemenz, *Principles of Colloid and Surface Chemistry*, 2nd Ed., Marcel Dekker, New York, 1986, pp. 534–539; A. W. Adamson, *Physical Chemistry of Surfaces*, 4th Ed., Wiley, New York, 1982, pp. 584, 594.
41. H. M. Sadek and J. Olsen, Pharm. Technol. **5,** 40, 1981.

42. W. Lowenthal and R. Burress, J. Pharm. Sci. **60,** 1325, 1971; W. Lowenthal, J. Pharm. Sci. **61,** 303, 1972.
43. S. J. Gregg and K. S. W. Sing, *Adsorption, Surface Area and Porosity,* Academic Press, New York, 1982; S. J. Gregg, *The Surface Chemistry of Solids*, 2nd Ed., Reinhold, New York, 1982, pp. 132–152.
44. J. J. Kipling, Q. Rev. **10,** 1, 1956.
45. R. E. Franklin, Trans. Faraday Soc. **45,** 274, 1949.
46. W. A. Strickland, Jr., L. W. Busse, and T. Higuchi, J. Am. Pharm. Assoc. Sci. Ed. **45,** 482, 1956.
47. A. Q. Butler and J. C. Ransey, Jr., Drug Standards **20,** 217, 1952.
48. B. S. Neumann, in H. S. Bean, J. E. Carless, and A. H. Beckett (Eds.), *Advances in Pharmaceutical Sciences*, **Vol. 2**, Academic Press, New York, 1967, p. 181.
49. E. N. Hiestand, J. Pharm. Sci. **55,** 1325, 1966.
50. C. F. Harwood and N. Pilpel, Chem. Process Eng. **49,** 92, 1968.
51. N. Pilpel, in H. S. Bean, A. H. Beckett, and J. E. Carless (Eds.), *Advances in Pharmaceutical Sciences*, **Vol. 3,**Academic Press, New York, 1971, pp. 173–219.
52. L.-E. Dahlinder, M. Johansson, and J. Sjögren, Drug Dev. Ind. Pharm. **8,** 455, 1982.
53. A. S. Arambulo, H. Suen Fu, and D. L. Deardorff, J. Am. Pharm. Assoc. Sci. Ed. **42,** 692, 1953.
54. A. M. Raff, A. S. Arambulo, A. J. Perkins, and D. L. Deardorff, J. Am. Pharm. Assoc. Sci. Ed. **44,** 290, 1955.
55. F. C. Hammerness and H. O. Thompson, J. Am. Pharm. Assoc. Sci. Ed. **47,** 58, 1958.
56. D. E. Fonner, Jr., G. S. Banker, and J. Swarbrick, J. Pharm. Sci. **55,** 181, 1966.
57. K. Ridgway and R. Rupp, J. Pharm. Pharmacol. **21 Suppl**., 30S, 1969.
58. G. Gold, R. N. Duvall, B. T. Palermo, and J. G. Slater, J. Pharm. Sci. **55,** 1291, 1966.
59. P. York, J. Pharm. Sci. **64,** 1216, 1975.
60. E. Nelson, J. Am. Pharm. Assoc. Sci. Ed. **44,** 435, 1955.
61. E. L. Parrott, Drug Cosmetic Ind. **115,** 42, 1974.
62. D. Train, J. Am. Pharm. Assoc. Sci. Ed. **49,** 265, 1960.
63. J. J. Fischer, Chem. Eng. **67,** 107, 1960.
64. B. S. Neumann, in J. J. Hermans (Ed.), *Flow Properties of Disperse Systems,* Interscience, New York, 1953, Chapter 10.
65. D. Train, J. Pharm. Pharmacol. **8,** 745, 1956; Trans. Inst. Chem. Eng. **35,** 258, 1957.
66. T. Higuchi et al., J. Am. Pharm. Assoc. Sci. Ed. **41,** 93, 1952; J. Am. Pharm. Assoc. Sci. Ed. **42,** 1944, 1953; J. Am. Pharm. Assoc. Sci. Ed. **43,** 344, 596, 685, 718, 1954; J. Am. Pharm. Assoc. Sci. Ed. **44,** 223, 1955; J. Am. Pharm. Assoc. Sci. Ed.**49,** 35, 1960; J. Pharm. Sci. **52,** 767, 1963.
67. E. L. Knoechel, C. C. Sperry, and C. J. Lintner, J. Pharm. Sci. **56,** 116, 1967.
68. J. A. Hersey, G. Bayraktar, and E. Shotton, J. Pharm. Pharmacol. **19,** 24S, 1967.
69. E. Shotton and D. Ganderton, J. Pharm. Pharmacol. **12,**87T, 93T, 1960; J. Pharm. Pharmacol. **13,** 144T, 1961.
70. J. Varsano and L. Lachman, J. Pharm. Sci. **55,** 1128, 1966.
71. S. Leigh, J. E. Carless, and B. W. Burt, J. Pharm. Sci. **56,**888, 1967.
72. J. E. Carless and S. Leigh, J. Pharm. Pharmacol. **26,** 289, 1974.
73. P. York and N. Pilpel, J. Pharm. Pharmacol. **24** (Suppl.), 47P, 1972.
74. J. Cooper and J. E. Rees, J. Pharm. Sci. **61,** 1511, 1972.
75. E. N. Hiestand, J. E. Wells, C. B. Peot, and J. F. Ochs, J. Pharm. Sci. **66,** 510, 1977.

Chapter Legacy

Fifth Edition: published as Chapter 19 (Micromeritics). Updated by Patrick Sinko.
Sixth Edition: published as Chapter 18 (Micromeritics). Updated by Patrick Sinko.